Link Adaptation Strategies for Cellular Downlink with low-fixed-rate D2D Underlay

A 3GPP LTE Case Study

Afonso Fernandes Lopes Marques Eduardo

Supervisors: António José Castelo Branco Rodrigues
Nuno Kiilerich Pratas
Petar Popovski

August 2014

Acknowledgement

I would like to thank all my colleagues, friends and family that supported me during this work. A special word of gratitude to my family that supported me emotionally and financially.

Likewise, I want to thank Prof. António Rodrigues for his friendship, mentorship and advice. Plus, a word of appreciation to Nuno Kiilerich which was a source of motivation, support and productive debate. Without both of them this work would be much harder to accomplish.

Finally, thanks to all the people from APNet, at Aalborg University, for their hospitality and much needed help. Specially, Prof. Petar Popovski.

Abstract

The new paradigm of Machine-to-Machine (M2M) communications poses problems in regards to the spectrum usage. In a situation where a massive number of devices wants to communicate, efficient Radio Resource Management (RRM) algorithms are of extreme importance. It might even occur that the number of devices to be served exceeds the number of available resources which reinforces the need to share those resources. Downlink with low-fixed-rate (Device-to-Device) D2D underlay and (Successive Interference Cancellation) SIC techniques are emergent solutions. The considered scenario can be described as a Base Station (BS) that is transmitting to a given User Equipment (UE), while a (Machine-Type Device) MTD is also communicating with the same UE, D2D link. Long Term Evolution (LTE) physical layer, Single-Input Single-Output (SISO) mode and block flat Rayleigh fading are assumed in both links. Only the BS is able to perform Link Adaptation (LA). In this context, the problem is to devise appropriate LA strategies that guarantee the feasibility of Interference Cancellation (IC). The author presents and evaluates two LA strategies that serve different purposes. One allows minimal outage operation despite limited information regarding the D2D link, while the other seeks to maximize the system efficiency at the cost of extra information.

Keywords: M2M, D2D Underlay, SIC, LTE, LA

Index

List of Figures

List of Tables

List of Abbreviations

3GPP	3rd Generation Partnership Project
5G	5th Generation
ACK	Acknowledgement
AWGN	Additive White Gaussian Noise
BLER	Block Error Rate
BS	Base Station or Cell
CB	Code Block
CCI	Co-Channel Interference
CDMA	Code Division Multiple Access
CoMP	Coordinated Multipoint
CP	Cyclic Prefix
CQI	Channel Quality Indicator
CRC	Cyclic Redundancy Check
CSI	Channel State Information
CW	Code Word
D2D	Device-to-Device
DLSCH	Downlink Shared Channel
eNodeB	Evolved Node B
EPC	Evolved Packet Core
E-UTRAN	Evolved-Universal Terrestrial Radio Access Network
FDD	Frequency Division Duplex
FFT	Fast Fourier Transform
HARQ	Hybrid Automatic Repeat Request
I2D	Infrastructure-to-Device
IC	Interference Cancellation
IDFT	Inverse Discrete Fourier Transform
IFFT	Inverse Fast Fourier Transform
LA	Link Adaptation

LTE	Long Term Evolution
M2M	Machine-to-Machine
MAC	Medium Access Control
MCS	Modulation and Coding Scheme
MIMO	Multiple-Input Multiple-Output
MTD	Machine-Type Device
NACK	Negative Acknowledgment
OFDM	Orthogonal Frequency-Division Multiplexing
PDCP	Packet Data Control Protocol
PDSCH	Physical Downlink Shared Channel
PHY	Physical (Layer)
QAM	Quadrature Amplitude Modulation
QoS	Quality of Service
RB	Resource Block
RE	Resource Element
RLC	Radio Link Control
RRC	Radio Resource Control
RRM	Radio Resource Management
SINR	Signal-to-Interference-plus-Noise Ratio
SNR	Signal to Noise Ratio
SIC	Successive Interference Cancellation
SISO	Single-Input Single-Output
TB	Transport Block
TDD	Time Division Duplex
TTI	Transmission Time Interval
UE	User Equipment
WSN	Wireless Sensor Network

List of Software

1. MATLAB R2013a
2. Vienna LTE Link Level Simulator v1.7r1089 (modified)

Chapter 1. Introduction

1.1. Motivation

As users increasingly turn to mobile broadband, mobile data traffic has been growing at an extraordinary rate. With the advent of new paradigms, such as the Internet of Things, mobile traffic is likely to reach even higher growth rates so much so that it is expected to grow nearly 11 fold by the end of 2018 when compared to that of 2013 [1]. This, in turn, poses many challenging problems as the wireless cellular networks have to evolve in order to accommodate this boom.

To date, wireless standards have been evolving so that they can achieve higher data rates, lower latencies and use the spectrum in a more efficient fashion. With such objectives in mind, these standards, namely the Long-Term Evolution (4G LTE) [2], make use of higher Modulation and Coding Schemes (MCS) that can be dynamically adjusted to cope with different channel conditions (also known as Link Adaptation – LA) such that a certain Quality of Service (QoS) can be guaranteed. In addition, LTE supports Multiple-Input Multiple-Output (MIMO) modes and standardizes multiple bandwidths and cell sizes which increase spectrum and latency flexibility.

Currently, the design of future 5th generation (5G) cellular networks is in the works and, within this framework, several technologies are being investigated. In [3], it is argued that a significantly better performance cannot be accomplished by simply adding new features to the existing standards and that such goal requires instead the introduction of disruptive technologies that force the deep-rooted cellular principles to be reformulated. Among those technologies, there are two that fall into the scope of this work: Device-to-Device (D2D) and Machine-to-Machine (M2M) communications.

Cellular networks of the previous generations were designed under the principle that the infrastructure, specifically the Base Station (BS) within each cell, is the controlling entity such that all the communications must go through it – Infrastructure-to-Device (I2D) communications. While this principle is reasonable in a voice-driven system in which the two parties are usually far from one another, the same might not be as good in an increasingly data-driven system. As a matter of fact, the situation where several devices within a cell want to share content is likely to occur often in the near future. In this scenario, if this very same premise was to be maintained, these devices would require multiple hops in order to communicate as opposed to a single hop if D2D communications were to be allowed. It should be noted that not only a lower latency could be achieved, but gains related to the amount of resources used and battery drain could be had. In addition, the use of such type of communications would also reduce the network management load even more so if a large number of connected devices were to be located within a single cell. D2D communication refers, thus, to the ability of one wireless device to communicate, via direct link, with another using the spectrum that is available for regular cellular communications. It is noteworthy that existing technologies, such as Wi-Fi and Bluetooth,

already allow devices to directly communicate with each other, but the usage of unlicensed radio resources leads to several limitations given that interference levels cannot be properly controlled.

On the other hand, M2M consists of a multitude of Machine-Type Devices (MTDs) connected to the network. These devices are often described in the context of Wireless Sensor Networks (WSNs) which are able to offer numerous applications related to data collection, ranging from smart-city communications to health-care and environmental monitoring. These services share the fact that are supported by low-data-rate communications, but have different requirements in regards to the number of supported devices, latency and reliability.

At this point, it is evident that D2D and M2M are closely related and that the potential synergies between the two should be exploited in the design of the future 5G cellular networks. One problem that arises is related to the spectrum usage. In fact, in a situation where a massive number of devices wants to communicate, efficient Radio Resource Management (RRM) algorithms are of extreme importance. In certain circumstances, it might even occur that the number of devices to be served exceeds the number of resources which further reinforces the emergence of Interference Cancellation (IC) techniques.

IC techniques allow a specified receiver to operate with higher levels of Co-Channel Interference (CCI), therefore the network can use the spectrum in a more efficient fashion by assigning the same resources to multiple links within a given cell. Thus, in a future cellular network, D2D and I2D communications are likely to coexist in the same time and spectrum.

In [4], it is explained that 3GPP, the entity responsible by the LTE standardization, is currently evaluating the D2D technology as an add-on in the form of a new LTE release version. Given that D2D is not a feature that is natively supported by LTE, it is important to limit its impact on the already existing networks. Therefore, in that context, it is assumed that these type of communications are to be performed within uplink carriers in FDD or uplink subframes in TDD. However, in the 5G networks, D2D is likely to be natively included and, in that sense, extending the option to be able to perform these communications during the downlink allows for a greater flexibility in resource management which might lead to a better performance.

Thus, it follows that this work focuses in the cellular downlink with low-fixed-rate D2D underlay. This scenario can be summarily described as a BS that is transmitting to a given User Equipment (UE), I2D link, while a MTD is also communicating with the same UE, D2D link. LTE physical layer and Single-Input Single-Output (SISO) mode is assumed in both links. Additionally, the D2D link operates at a fixed-low data rate, whereas the I2D link is able to perform LA. In this context, the problem is to devise appropriate link adaptation strategies to guarantee the feasibility of IC and, thus, ensure that the system behaves properly.

The author presents and evaluates two LA strategies that serve different purposes. One allows the system to reliably operate with limited information regarding the D2D link, while the other seeks to maximize the system efficiency at the cost of extra information.

1.2. Goals and Project Contribution

The study's main contribution is twofold. First, the author investigates the possible SIC techniques that can be applied in a D2D and I2D coexistence scenario while focusing on the LTE physical layer. In this stage, a survey of the existing IC techniques is performed. These findings are then used to design a D2D-enabled device and its performance is evaluated under a cellular downlink with low-fixed-rate D2D underlay scenario. It should be noted that this scenario contrasts to that of the mainstream, where D2D underlay only operates during the uplink, as it is believed that also using the cellular downlink leads to an overall better performance because it adds an increased flexibility that RRM algorithms can exploit.

The other contribution encompasses the presentation and evaluation of two LA strategies to be applied at the BS. The first strategy aims to guarantee the reliability of the system under the aforementioned scenario. The strategy itself was originally developed in [5] as a means to achieve zero-outage in a theoretical system. The approach here devised differs in the sense that the LTE physical layer is considered which naturally introduces limitations in regards to its applicability and performance. The other LA strategy aims to maximize the system efficiency at the cost of extra information at the BS side, namely Channel State Information (CSI) of I2D and D2D links.

It is noteworthy that the system under evaluation is SISO and the channel can be described as a block flat Rayleigh fading channel. However, during this study, it is given some insight as to how these strategies can also be applied to frequency selective channels.

Chapter 2. Technical Approach

1.1. Introduction

In this section, the author first presents concepts that are necessary to understand the work exposed in this report. That said, a brief description of the LTE standard is presented, focusing on the physical layer procedures. Interference Mitigation (Cancellation) techniques, namely SIC, are then discussed after which a survey regarding IC techniques applied to OFDM systems, such as LTE, is conducted.

The last subsection focuses on LTE-applicable Link Adaptation strategies for the considered cellular downlink with low-fixed-rate D2D underlay scenario. Two strategies are discussed: zero-outage rule and weighted rule.

2.1. 3GPP Long Term Evolution

2.1.1. LTE Network Architecture basics

The network architecture consists basically of three parts: the User Equipment (UE), the Evolved Universal Terrestrial Radio Access Network (E-UTRAN) and, lastly, the Evolved Packet Core (EPC) [2]. Figure 1 depicts a simplified model of the LTE network and its relation with previous generation networks.

The UE is a device used by an end-user and whose purpose is to communicate. Such device can be, for instance, a hand-held telephone or a laptop.

The E-UTRAN is the LTE radio access network and consists of several BSs, termed eNodeBs. The BSs are responsible for hosting the physical (PHY), Medium Access Control (MAC), Radio Link Control (RLC), Packet Data Control Protocol (PDCP) and Radio Resource Control (RRC) layers. BSs can, thus, dynamically schedule and allocate radio resources to UEs during the uplink and downlink.

The EPC is the LTE core network but, since it goes beyond the focus of this work, it suffices to say that is responsible for managing the E-UTRAN.

Figure 2 shows the LTE layer structure and its main functions. For a more detailed description, the reader is referred to [6], [7].

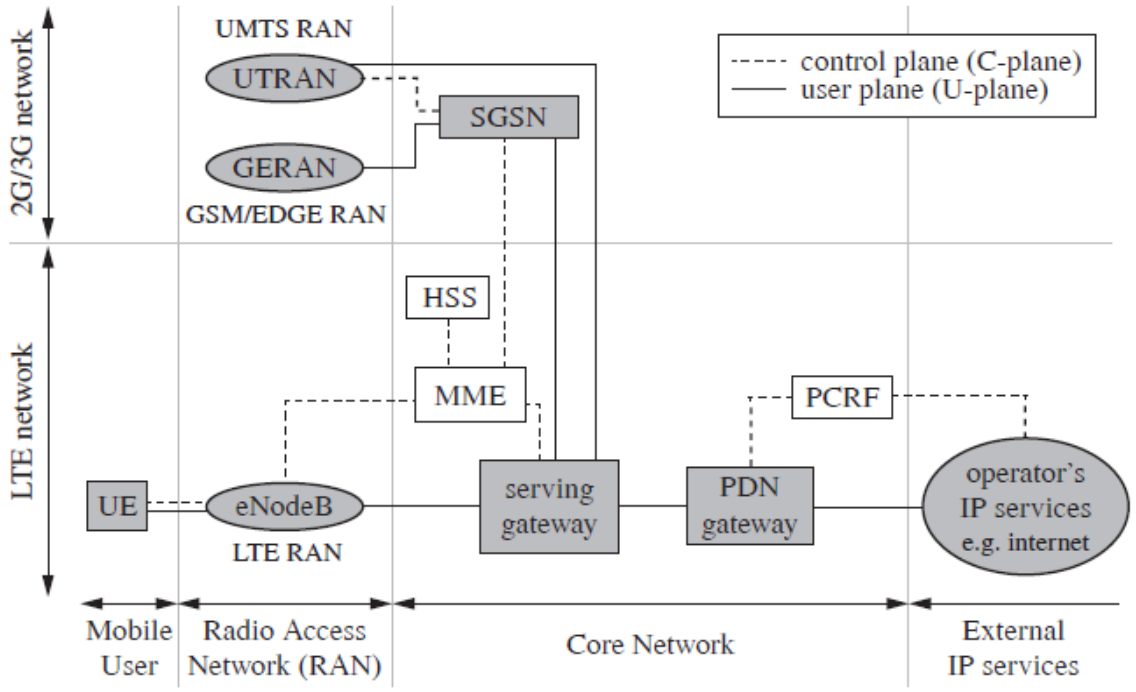

FIGURE 1. SIMPLIFIED LTE ARCHITECTURE

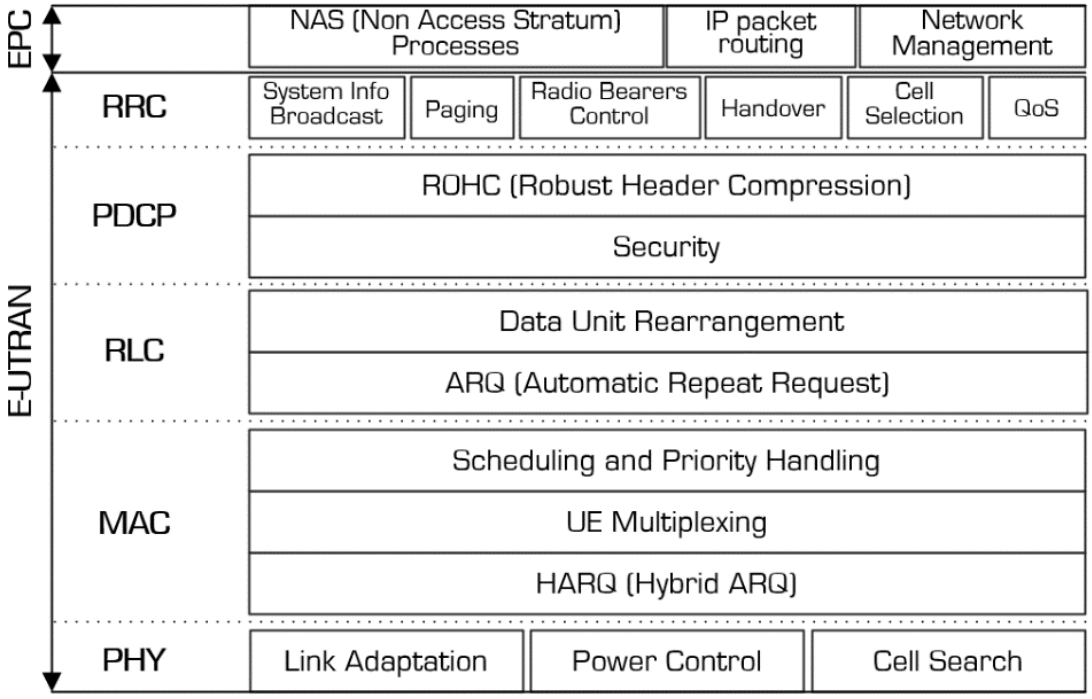

FIGURE 2. LTE LAYER STRUCTURE

2.1.2. LTE Physical Layer

2.1.2.1. Time-Frequency Representation

The LTE physical layer uses Orthogonal Frequency-Division Multiplexing (OFDM), meaning that radio resources span in time and frequency domains.

In the time domain, LTE arranges the transmission into radio frames whose length is 10ms. Each radio frame is subdivided into ten subframes of 1ms (TTI), subsequently composed of two slots of length 0.5ms each. One slot, in turn, consists of six or seven OFDM symbols depending on whether a normal or extended cyclic prefix is used. The purpose of this prefix is to avoid inter-symbol interference and it is added to the beginning of each symbol. It is convenient to note that only the normal CP is considered throughout this work.

One of the requirements, when standardizing, was spectrum flexibility and, as such, LTE has a list of spectrum allocations that range from 1.4 to 20 MHz. The bandwidth itself is divided into equally-spaced orthogonal subcarriers whose typical spacing is 15 kHz. Each subcarrier group, 12 consecutive subcarriers for this specific configuration, has a total bandwidth of 180 kHz and it is often known as a Resource Block (RB). Table 1 presents the set of possible bandwidths along with other parameters arising thereof [2].

If one combines the time and frequency domains, a resource grid is obtained and each basic element is named Resource Element (RE) as observed in Figure 3. The x-coordinate of a RE specifies the OFDM symbol to which it belongs in the time domain, and its y-coordinate the OFDM subcarrier in the frequency domain.

At this point, it should be noted that downlink and uplink have different physical channels. Therefore, control, reference and data signals are organized in a different fashion. In this study, only the downlink transmission is considered. However, explaining how these signals are assigned into the resource grid goes beyond the scope of this work. Such information can be found in e.g. [8] for a more intuitive description. Another consideration is that the frame structure differs depending on which duplex scheme is being used: Frequency-Division Duplex (FDD) or Time-Division Duplex (TDD). Type 1 frame structure, used in FDD mode, is assumed throughout this study.

TABLE 1. STANDARDIZED LTE BANDWIDTHS

Channel Bandwidth $(\boldsymbol{BW})$ [MHz]	**1.4**	**3**	**5**	**10**	**15**	**20**
Number of RBs	6	15	25	50	75	100
Number of data subcarriers	72	180	300	600	900	1200
Transmission Bandwidth [MHz]	1.08	2.7	4.5	9	13.5	18
Bandguard size $(\%\ \mathbf{of}\ \boldsymbol{BW})$	23	10	10	10	10	10

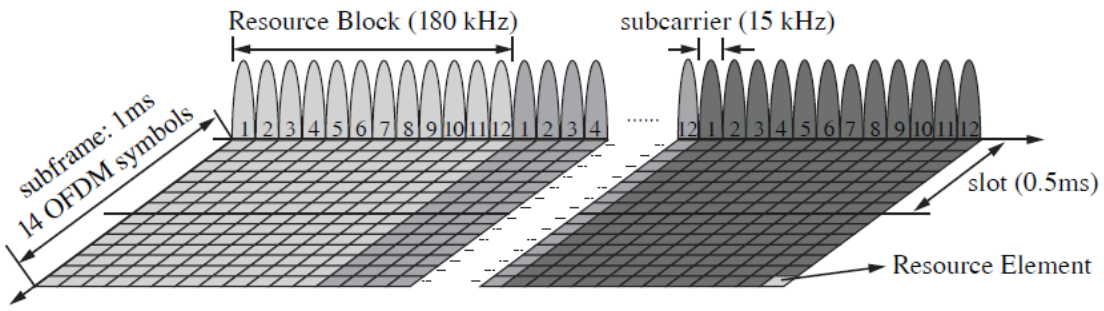

FIGURE 3. RESOURCE GRID

2.1.2.2. Downlink Signal Processing

The simplified chain of downlink signal processing procedures is depicted in Figure 4 [8]. This chain results of the combination of Downlink Shared Channel (DLSCH) and Physical Downlink Shared Channel (PDSCH) processing.

DLSCH is the main downlink transport channel type in LTE and is responsible for carrying information related to user data, dedicated control information and other downlink system information. All this information, belonging to a specific user, is grouped into chunks of variable length known as Transport Blocks (TBs). Its further processing encompasses TB-CRC (TB - Cyclic Redundancy Check) attachment, Code Block (CB) segmentation, CB-CRC insertion, turbo coding, rate matching and CB concatenation.

The processing chain begins by calculating and attaching a 24-bit CRC to each TB as a means to detect errors at the receiver side. The CRC-attached TB may be split into several CBs since the turbo coder interleaver has a maximum size of 6144 bits. In such case, each CB is attached with its own 24-bit CRC (CB-CRC). Subsequently, each CRC-attached CB is rate-1/3-turbo-code encoded followed by a rate matching procedure which includes additional interleaving and produces CB Code Words (CWs) with the desired code rate. The CB-CWs are then concatenated to form a TB-CW, completing the DLSCH processing phase and moving to the PDSCH processing stage. A complete specification of this processing can be found in [9].

The next stage, PDSCH processing, is responsible for converting the bit stream coming out of DLSCH processing into radio frame data to be transmitted by each antenna. Its first operation is to scramble the CW with a Gold scrambling sequence. It should be noted that the generated scrambling sequences are unique to neighboring cells, based on their PHY level identity, so that the interference is randomized and transmissions from adjacent cells can be separated before decoding. After the scrambler procedure, the scrambled CW passes through a symbol mapper whose modulation can be 4-, 16- or 64-QAM depending on the Modulation and Coding Scheme (MCS) index. The selection of this index and, therefore, the modulation to be applied will be addressed in a subsequent subchapter. The

following steps, layer mapping and precoding, relate to MIMO transmissions where multiple transmit antennas are present. In such scenario, up to two CWs can be transmitted simultaneously. Layer mapping is thus the procedure that assigns the CWs to layers, depending on the selected transmission mode. Precoding then combines the information in such layers and generates a sequence for each antenna port. Next, each sequence is mapped to REs that form the resource grid which, in turn, serves as input to the OFDM modulator, producing the baseband time-domain signal to be transmitted by each antenna after radio-frequency upconversion. For a more detailed specification, the reader is referred to [10].

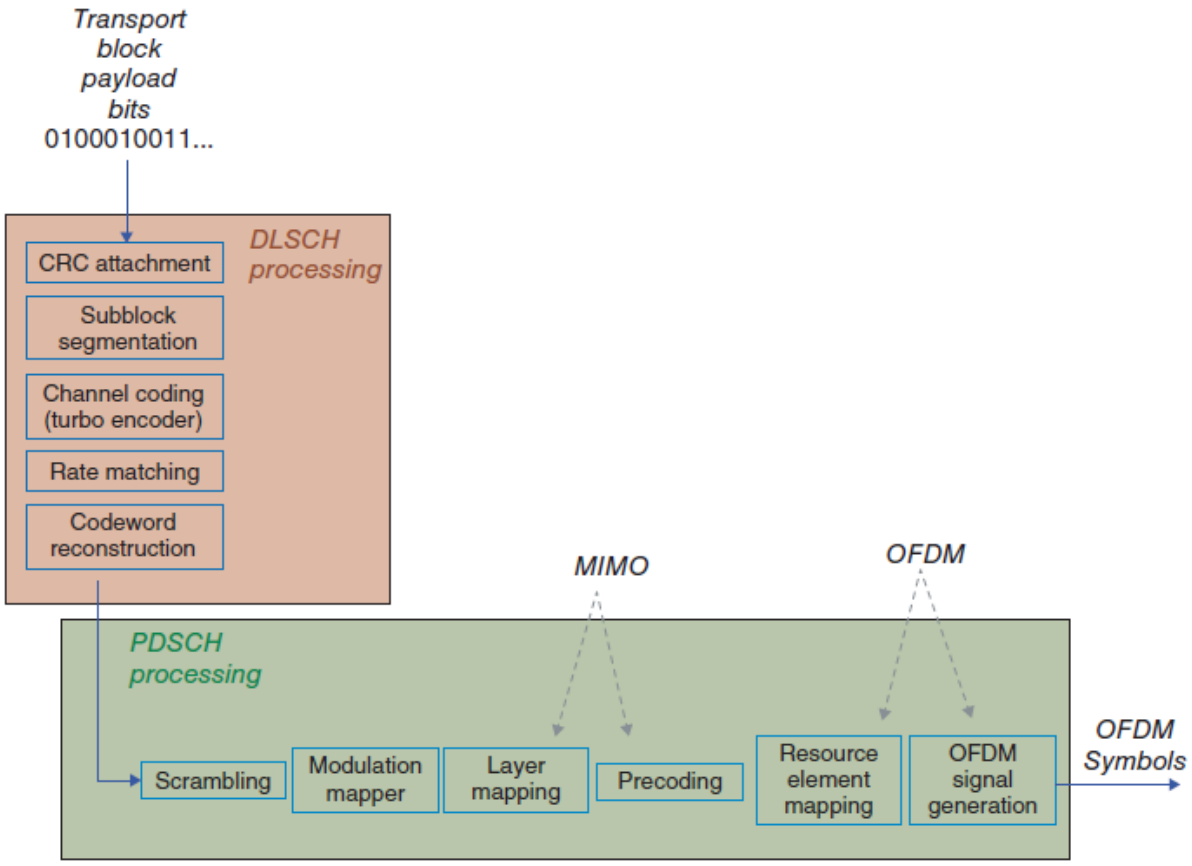

FIGURE 4. DOWNLINK SIGNAL PROCESSING CHAIN

2.1.2.3. OFDM Transmission and Reception

As previously described, the downlink transmission is based on an OFDM scheme. This procedure operates on the resource grid by taking the QAM modulated symbols column wise and performing an IFFT operation followed by CP addition to generate the OFDM modulated signal.

Assume a subcarrier spacing Δ_f, each subcarrier f_k is thus considered as follows:

$$f_k = k\,\Delta_f\,,\ \ k = 0, 1, \ldots, N-1, \tag{1}$$

where N corresponds to the number of subcarriers used. The sampled OFDM symbol $x[n]$ can then be expressed as [11]:

$$x[n] = \sum_{k=0}^{N-1} X[n]|_{f_k}, \quad X[n]|_{f_k} = X[k]\, e^{j2\pi k\frac{n}{N}},\ n = 0, 1, \dots, N-1, \qquad \textbf{(2)}$$

where $X[n]|_{f_k}$ denotes the f_k subcarrier component and $X[k]$ the corresponding QAM symbol. Note that equation (2) is the N-point IDFT of the QAM symbols (taken column wise) and can be computed by the IFFT algorithm. This procedure is then followed by CP addition, extending the duration of the OFDM symbol by copying its last samples into its front

In a multipath fading channel, without AWGN, consisting of M paths with d_m delays and an impulse response h, the received OFDM signal, in the time domain, is [8]:

$$y[n] = \sum_{m=0}^{M} h[m]\, x[n - d_m]. \qquad \textbf{(3)}$$

Assuming that the CP length is greater or equal than the maximum path delay, then the orthogonality between consecutive OFDM symbols is preserved which, in turn, allows the post-FFT received signal at a given subcarrier f_k to be written, in the frequency domain, as [8]:

$$Y_{postFFT}[k] = H[k]X[k], \quad H[k] = \sum_{m=0}^{M} h[m]\, e^{-\frac{j2\pi k d_m}{N}}, \qquad \textbf{(4)}$$

where $H[k]$ is the complex gain of the channel at subcarrier f_k. This expression indicates that the effects of multipath fading can be removed (or, at least, mitigated) at the receiver side by using a frequency-domain equalization whose channel gain estimates $\widehat{H}_k$ are obtained from reference signals.

2.1.2.4. Adaptive Feedback

In order to achieve a better performance, LTE introduces flexibility in regards to its transmission parameters based on the received channel conditions. There are three parameters worth mentioning: Rank Indicator, Precoding Matrix Indicator and Channel Quality Indicator (CQI). The first two are used when MIMO transmission occurs and, since this study focuses on SISO mode, CQI is the only indicator to be addressed in this subsection.

The CQI is a measurement index that allows the receiver to report the downlink radio channel quality, specifying the modulation constellation and coding rate that best fit the measured link quality. This index signals, on a per-codeword basis, the highest of 15 standardized MCSs that guarantees a BLER lower or equal to 10% [12]. Since the selection of the CQI is to be performed at the receiver side, it is a procedure that is not standardized, being the device manufacturer responsibility to conceive a

method that allows the device to exploit the channel conditions in the best possible fashion. However, this field has already been the subject of extensive studies and the current practice is to obtain a mapping between the 10% point of the BLER curve of the corresponding MCS (threshold) and each CQI, a method known as SINR-to-CQI mapping. Note that this mapping is receiver-specific in the sense that a better receiver might achieve a similar BLER at a lower SINR for a given MCS.

Another issue that arises relates to the channel model, namely frequency-selective fading channels. In this type of channels, as opposed to block fading channels, distinct RBs generally experience different SINRs, but the CQI reports the quality on a per-codeword basis. It is then of utmost importance to conceive an abstraction of the channel model. Luckily, several studies have already addressed this issue and [13] provides a succinct, yet comprehensive analysis. In summary, to overcome this problem, the SINR-to-CQI mapping is obtained from a SISO AWGN simulation and an effective post-equalization SINR, based on a compression method that factors in the SINRs from the assigned RBs, is computed such that there is a close match between the BLERs of the equivalent AWGN channel and the real fading channel.

2.1.3. Interference Mitigation Techniques

2.1.3.1. Introduction

As the amount of users increases, there is a need to use the spectrum in a more efficient fashion. Interference mitigation techniques emerge as a promising solution allowing users to share the spectrum. These techniques can be categorized into two types depending on the entity that is in control of performing such operations.

One is applied at the transmitter side and requires the knowledge of CSI which, in turn, imposes several limitations in a real scenario as this information can only be tracked by such devices if the fading conditions are relatively slow (feedback delay). Despite such limitations, CoMP (Coordinated Multipoint) transmission arises in the context of LTE-Advanced and is an example of such technique. It was developed as a means to mitigate interference and thus improve the performance at the cell edge by giving neighboring BSs the ability to transmit in a coordinated fashion [14], [15].

In the context of this study, cellular downlink with low-fixed-rate D2D underlay, the first option is not feasible since the transmit entities (MTD and BS) are not able to coordinate their transmissions in such way. Luckily, the other type of interference mitigation relies on receiver-based solutions which, naturally, does not involve an accurate CSI at the transmitter, at the cost of an increased computational complexity. One of such techniques is data Interference Cancellation (IC).

Unlike CDMA systems, OFDM systems, such as LTE, do not use spreading, therefore extracting the signal of an interferer by means of channel decoding is generally the only processing gain available [16]. It is precisely in this circumstance that the concept of Successive Interference Cancellation arises.

2.1.3.2. Successive Interference Cancellation

2.1.3.2.1. Principle

The idea of SIC is to decode different users sequentially such that the interference due to the decoded users is subtracted before decoding the other users.

In order to further illustrate this principle, consider a scenario where two entities are transmitting. The received signal is composed by signal I, to be regarded as a strong interference, and signal D, as the desired encoded signal. In such case, the receiver decodes the received signal in two stages as seen in Figure 5. First, it decodes I while treating D as Gaussian interference. The interference is then reconstructed by re-encoding the detected message and multiplying it by the estimated channel response. This estimated interfering signal is then subtracted, on a symbol basis, from the detected signal such that, in an ideal case, the resulting signal only consists of the desired encoded signal (D); therefore, the ability of the receiver to be able to successfully decode the message is improved.

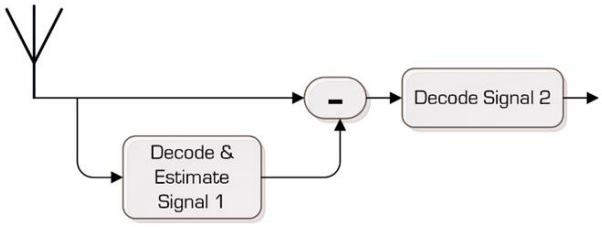

FIGURE 5. SIC PRINCIPLE

This technique can achieve a significantly higher performance when compared to a system where no SIC is applied, especially so when the interference is significantly stronger than the intended signal. Actually, in the latter, the maximum achievable rate (normalized) under AWGN conditions is [17]

$$C_{noSIC} = \log_2\left(1 + \frac{P_D}{P_I + \sigma_w^2}\right) = \log_2(1 + SINR_D), \quad \textbf{(5)}$$

while in the former, after successful IC, is

$$C_{SIC} = \log_2\left(1 + \frac{P_D}{\sigma_w^2}\right) = \log_2(1 + SNR_D), \quad \textbf{(6)}$$

where P_I, P_D denote the received power of I and D respectively and σ_w^2 refers to the Gaussian noise power. It thus follows that $C_{SIC} \geq C_{noSIC}$.

It should be noted, however, that SIC is not always applicable. First, let Γ_I and Γ_D denote the thresholds below which the receiver is not able to decode signals I and D respectively. These thresholds, in turn, depend mainly on the MCS used to encode a given signal such that a low MCS corresponds to a lower threshold. There are four regions of operation worth mentioning:

- $SINR_D > \Gamma_D$: The receiver does not need to apply SIC in order to decode D.
- $SINR_D < \Gamma_D$ and $SINR_I = \frac{P_I}{P_D+\sigma_w^2} < \Gamma_I$: The receiver cannot apply SIC nor can decode D. Outage occurs.
- $SINR_D < \Gamma_D$, $SINR_I = \frac{P_I}{P_D+\sigma_w^2} > \Gamma_I$ and $SNR_D < \Gamma_D$: The receiver can apply SIC, but it still cannot decode D. Outage occurs.
- $SINR_D < \Gamma_D$, $SINR_I = \frac{P_I}{P_D+\sigma_w^2} > \Gamma_I$ and $SNR_D > \Gamma_D$: The receiver needs to apply SIC in order to decode D.

From this analysis, it follows that SIC works best when low MCSs are used to encode I and/or D, which is consistent with the cellular downlink with low-fixed-rate D2D underlay scenario. It is also noteworthy that the SIC concept can be applied to several interferers, but as shown in [18], most of its throughput gain is obtained by cancelling a single interferer.

2.1.3.2.2. Strategies

In the literature there are several approaches to SIC, however, when it comes to OFDM systems, there are two general types based on how the symbol estimates for cancellation are devised.

In the Hard SIC, the cancellation is based on a hard decision symbol estimate which means the estimates take values from one of the modulation constellation points. In such case, if there are too many decision errors in the estimate, this strategy could worsen the performance compared to not using SIC. Therefore, when adopting this technique, SIC is only performed when a CRC checks which, in LTE, can either be the one belonging to a CB or the TB. In [19], both approaches were tested and the Hard SIC receiver based on CB CRC has practically no gain over the one based on TB CRC. Thus, it is more efficient to use the latter.

On the other hand, in the Soft SIC, the cancellation is based on soft decision symbol estimates which are based on bit likelihood values provided by the decoder. This type of decoders provide an increase in performance when compared with Hard SIC at a cost of higher complexity [19].

2.1.4. Link Adaptation Strategies

2.1.4.1. Introduction

As previously explained, SIC is an interference mitigation technique. However, it can also be considered as a multiple packet reception scheme for it allows various users to share the same resources. In fact, if one is to interpret the interferers as yet other sources of useful information (from other devices), one can readily understand that SIC permits the coexistence of multiple links.

SIC is therefore an extremely useful tool, especially so in the cellular downlink with low-fixed-rate D2D underlay scenario that is being considered in this study where a given BS is transmitting to a specified UE (I2D link) while a MTD is also communicating with the same UE, D2D link (refer to subsection 3.2 for a more exhaustive description). It thus follows that in order for this system to operate in an appropriate fashion, LA strategies are paramount. As described in subsection 2.1.3.2.1, SIC is not always applicable and, thus, in this context, LA strategies appear not only as a means to adapt the link to the fading conditions, but also to limit the SIC outage regions.

In the following subsections, the focus is on LA strategies applicable to LTE specifically tailored to this cellular downlink with low-fixed-rate D2D underlay scenario where only the I2D link is adaptation-capable. Another consideration, and as explained in subsection 2.1.2.4, is that LA in LTE is the process of selecting the MCS based on the CQI (SISO mode). It thus follows that the presented strategies focus on devising receiver-sided rules to select the CQI that is to be reported to the BS.

2.1.4.2. SIC Zero-outage Rule

In order to devise a rule, an objective must be set. One such goal can be to meet an outage as low as possible. It is, precisely in this context, that zero-outage rule arises.

This strategy was originally developed in [5] for several scenarios, including the one that is being considered in this study (referred as single-user decoding, single MTD). In [5], the focus is on a purely theoretical system in which the transmitters are able to use capacity-achieving random Gaussian codebooks. In LTE, however, there is a discrete number of available MCS, therefore it is expected that adjusting and applying this rule to LTE, zero-outage is unlikely to be achieved, but it can be significantly reduced.

Another important aspect is that this rule was developed bearing in mind that adaptation does not have to necessarily rely on the receiver feedback. In fact, it does not require knowing the CSI about the D2D link and the CSI of the I2D (the link to adapt) can be inferred at the transmitter, during the upload frames, by exploiting the channel symmetry property if a TDD scheme is employed. It is noteworthy that the latter assumption poses several limitations because, if fast fading occurs or a FDD scheme is used, I2D CSI inference is not accurate. Still, the single fact that there is no need to know D2D CSI is in itself of great utility, specially so in the context of M2M communications where MTDs

might exhibit intermittent activity, rather than continuous. The receiver is only able to report the CSI estimate if transmission occurs given that this estimate is calculated from reference signals. Thus, in such scenarios, the receiver can report an accurate I2D CSI due to continuous transmission, but, since D2D communications occur intermittently, the reported D2D CSI can be fairly outdated, reporting, in a fast fading channel, an estimate that might be highly inaccurate.

Following the approach devised in [5], for the theoretical system, all transmitters use a capacity-achieving random Gaussian codebooks such that the maximal achievable rate (normalized) of a link i, R_i, with a given instantaneous SNR, SNR_i, is

$$R_i = \log_2(1 + SNR_i) = C(SNR_i). \quad \textbf{(7)}$$

One can also compute the minimal required SNR, Γ_i, that the link i must have such that the receiver is able to decode the signal successfully in an interference-free scenario by taking

$$\Gamma_i = 2^{R_i} - 1 = C^{-1}(R_i). \quad \textbf{(8)}$$

It thus follows that, in downlink with low-fixed rate D2D underlay scenario, the maximal downlink transmission rate (I2D link), R_B, that is always decodable by the receiver is given by [5]

$$R_B = C\left(\frac{SNR_B}{1 + C^{-1}(R_M)\,(1 + SNR_B)}\right), \quad \textbf{(9)}$$

where SNR_B denotes the I2D instantaneous SNR and R_M is the D2D link rate. That said, it should be noted that R_M is fixed, therefore the BS does not need to know any instantaneous information regarding the D2D link in order to adapt its MCS.

Unlike this theoretical system in which there is a one-to-one relationship between R and a given MCS, due to Gaussian codebooks; in LTE, this relationship does not exist given that the number of available MCS is limited. There is thus a need to replace the C function by a heuristic mapping. Such mapping can be, as explained in subsection 2.1.2.4 and recalling that a given CQI translates into a specific MCS, the SINR-to-CQI mapping. In the SINR-to-CQI mapping, each MCS has a given threshold that is determined via simulation so that the receiver exhibits a 10% BLER. Let K denote the number of available MCSs and Γ_k denote the threshold associated to the kth MCS such that a higher MCS index corresponds to a more efficient (and less robust) MCS and therefore a threshold value that is also higher. Thus, this rule can be applied by the LTE SIC-capable receiver according to the following pseudo-code

1. $\Gamma_M = \text{get\_threshold}(\text{MCS}_\text{M})$ // fixed MTD MCS – known *a priori*
2. **for** new SNR_B **do** // new channel conditions (I2D)
3. $\text{SINR}_\text{eff} = \frac{\text{SNR}_\text{B}}{1+\Gamma_\text{M}(1+\text{SNR}_\text{B})}$ // effective SINR_B
4. $\text{CQI\_idx} = 1$
5. **for** $k = 2, \dots, K$ **do** // find the highest MCS that satisfies effective SINR_B
6. **if** $\text{SINR}_\text{eff} \leq \Gamma_k$ **then**
7. $\text{CQI\_idx} = k$
8. **end if**
9. **end for**
10. report(CQI_idx)
11. **end for**

FIGURE 6. ZERO-OUTAGE RULE

:

2.1.4.3. SIC Weighted Rule

Another possible goal is to maintain a balance between the outage probability and the overall throughput of the system. LTE physical layer defines a target BLER that is 10%, therefore, in this rule, the objective is to maximize the I2D throughput while satisfying the 10% BLER constraint at both links.

To tackle this problem, rather than trying to devise an optimal rule, a heuristic procedure based on the SIC concept is presented. First, it is assumed the knowledge of CSI of both links at the receiver. Knowing this information, the receiver can then evaluate if the D2D signal is decodable without applying SIC at least 90% of the time such that the target BLER is satisfied. This evaluation is done by comparing the instantaneous SINR of the D2D link, $SINR_M$, with its MCS threshold (which is fixed at all times), Γ_M. If its decodability rate satisfies the constraint, then when adapting the MCS of the I2D link, one can assume that the interference caused by the D2D link can be removed by means of SIC and thus, instead of using the SINR of the I2D link, $SINR_B$, to determine which MCS matches the best, one uses SNR_B.On the other hand, if the former condition is not satisfied, $SINR_B$ is used such that the I2D signal can be decoded without the need of SIC.

Following the same notation presented in the previous subsection, this rule can be summarized as:

1. $\Gamma_M = \text{get\_threshold}(\text{MCS}_\text{M})$ // fixed MTD MCS – known *a priori*
2. **for** new $\text{SINR}_\text{M}, \text{SINR}_\text{B}, \text{SNR}_\text{B}$ **do** // new channel conditions (I2D and D2D)
3. **if** $\text{SINR}_\text{M} \geq \Gamma_M$ **then** // determine effective SINR_B
4. $\text{SINR}_\text{eff} = SNR_B$
5. **else**
6. $\text{SINR}_\text{eff} = \text{SINR}_\text{B}$
7. **end if**
8. $\text{CQI\_idx} = 1$
9. **for** $k = 2, \dots, K$ **do** // find the highest MCS that satisfies effective SINR_B
10. **if** $\text{SINR}_\text{eff} \leq \Gamma_k$
11. $\text{CQI\_idx} = k$
12. **end if**
13. **end for**
14. report(CQI_idx)
15. **end for**

FIGURE 7. WEIGHTED RULE

Chapter 3. Scenario Description and Simulator Specification

3.1. Introduction

In this chapter, the concept of cellular downlink with fixed-low-rate D2D underlay scenario is described at both link and system level. Additional assumptions are presented.

The rest of the chapter focuses on the implementation of the link-level and system-level simulators and the description of the parameters that were considered in the simulations presented in the next chapter.

3.2. Scenario Overview

3.2.1. Link Level Description

Consider the topology depicted in Figure 8 which consists of two Single-Input Single-Output (SISO) links. The link denoted by D2D refers to the transmission of the MTD data to a given UE, whereas the I2D targets the same UE, but has the BS as the transmitting entity. The D2D is considered to be a low-rate link when compared to the I2D and, given that both are assumed to use the same time-frequency resources the former has, in general, a lower channel-coding rate. It is also assumed that the BS is able to dynamically adjust its rate as opposed to the MTD which operates at a fixed rate.

Another assumption is that the system operates under non-line-of-sight conditions such that these links are characterized by two independent block flat Rayleigh fading channels whose gains remain constant over a certain transmission time interval (TTI), which is considered to be equal to the length of one LTE subframe, and over all the assigned subcarriers. Furthermore, it is assumed that the UE has perfect CSI knowledge so much so that no estimation error arises when determining the channel gain estimates and the noise power. For LA purposes, the UE computes the CQI to be reported to the BS according to a given rule. In turn, this CQI report is assumed to occur in an instantaneous fashion so that the BS can apply the most appropriate MCS for each instantaneous channel realization. It should be noted, that in a real scenario, rather than instantaneous, the CQI report is periodic, but if one considers that the fading is sufficiently slow, the reports are still accurate enough, validating the simplification. Notice, however, that, for fast fading channels, this simplification no longer applies and those report parameters need to be modelled accordingly.

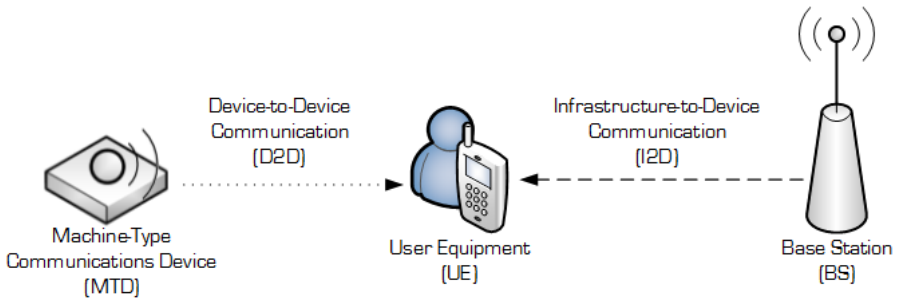

FIGURE 8. LINK-LEVEL TOPOLOGY

Since the goal is to evaluate the behavior of a SIC LTE receiver under the aforementioned scenario, let the complex baseband received signal at a given subcarrier, f_k, be defined in the frequency domain as

$$Y[k] = H_M[k]X_M[k] + H_B[k]\,X_B[k] + w, \tag{10}$$

where $X_M[k]$ and $X_B[k]$ are the complex baseband signals transmitted on subcarrier f_k by the MTD and BS respectively; $H_M[k]$ and $H_B[k]$ are the complex coefficients on subcarrier f_k of the two independent channels such that $H_M[k], H_B[k] \sim \mathcal{CN}(0, 1)$ and n represents the complex Gaussian noise: $w \sim \mathcal{CN}(0,\ \sigma_w^2)$. It is noteworthy that $E[|H_M(k)|^2] = E[|H_M(k)|^2] = 1$. Therefore, the expected SNR of both links on subcarrier f_k can be written as

$$E[SNR_i[k]] = E\left[\frac{|H_i[k]|^2 P_i}{\sigma_w^2}\right] = \frac{P_i}{\sigma_w^2}\ , i \in \{M, B\}, \tag{11}$$

where $P_i = E[|X_i[k]|^2]$ is the average transmitted power of the respective entity (MTD or BS).

At this point, it is also convenient to introduce the expected SINR on subcarrier f_k of both links as

$$E[SINR_i[k]] = E\left[\frac{|H_i[k]|^2 P_i}{\sigma_w^2 + \left|H_j[k]\right|^2 P_j}\right] = E\left[\frac{SNR_i[k]}{1 + SNR_j[k]}\right], (i,j) \in \{M, B\}^2\ , i\ \neq j\ . \tag{12}$$

Furthermore, particularizing for a flat fading channel, $H_i[k] = H_i[u]$, $\forall_{(k,u)}$. Consequently, all subcarriers experience the same instantaneous (and, hence, estimated) SNR and SINR, meaning that the k index can be dropped.

3.2.2. System Level Description

3.2.2.1. METIS Framework

The METIS project aims to provide technical analysis for future wireless systems often referred to as 5G [20]. The project defines several simulation cases in which the proposed systems are to be evaluated. This framework not only describes the possible environmental models, but also specifies the deployment of the network infrastructure along with the propagation, traffic and mobility models.

For this project, the case considered to be of most importance is referred as the dense urban information society (TC2) whose environment consists of a grid model based on the city structure of Madrid that, according to the METIS consortium, provides a more realistic non-homogenous building layout than the Manhattan grid and is, thus, capable of capturing real life effects more accurately. The reader is advised to consult [21] for an in-depth description.

3.2.2.2. System Level Scenario: Indoor on-body MTD

The building layout considered for this scenario is depicted in Figure 9 and it consists of four 8-floor square buildings. The BS is placed in the southwest corner of the roof of building 2. On the other hand, the user (UE) is inside building 3 and is stationary during each measurement, but, for each floor, it picks several different positions that are uniformly distributed. Additionally, this user has an on-body sensor (MTD) which directly communicates with the corresponding UE. It is assumed that the only source of interference is caused by the fact that the D2D link can share the same resources as the I2D link.

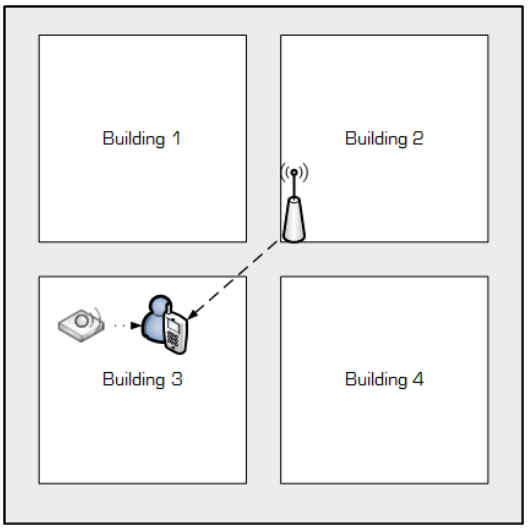

FIGURE 9 SYSTEM-LEVEL LAYOUT

3.3. Simulator Specification

3.3.1. Introduction

In this subsection, the implemented simulator is specified. The link level simulator is based on a publicly available LTE simulator [22]. Thus, the information here presented focuses on the modifications that were applied to that particular simulator along with the specification of simulation parameters.

It should be also noted that no calibration procedure had to be conducted since the original LTE simulator was already proved to be LTE standard compliant [22] [23].

3.3.2. Link Level Model

3.3.2.1. Overview

The link-level simulator consists of two transmitters and one SIC-capable receiver (see the following subsections for a detailed characterization). Recalling the scenario described in 3.2.1, it then follows that the transmit entities are the MTD and BS, while the UE is modelled by the receiver. Each link has an independent channel which is characterized as being a block flat Rayleigh fading channel. Table 2 specifies other simulation parameters.

TABLE 2. LINK LEVEL SIMULATION PARAMETERS

Parameters	Value
Number of transmitters	2
Number of receivers	1
Transmit mode	SISO
Available MCSs	27
Retransmissions (*HARQ*)	Not Supported
Bandwidth ($\boldsymbol{BW}$)	1.4 MHz
Number of RBs ($\boldsymbol{N_{RB}}$)	6
Number of subcarriers/RB	12
Number of data-assigned subcarriers ($\boldsymbol{N_{tot}}$)	72
Channel Type	Flat Rayleigh
Filtering	Block Fading
Subframe duration ($\boldsymbol{TTI}$)	1 ms
Frame size	10 TTIs
Simulation length	5000 TTI
OFDM symbols / TTI	14
Subcarrier Spacing ($\boldsymbol{\Delta_f}$)	15 kHz
CP length	Normal
Number of FFT points ($\boldsymbol{N_{fft}}$)	128

3.3.2.2. Channel Model

In order to implement the link-level propagation model (small-scale fading and noise) the following approach was adopted. First, recall that, in a multipath fading channel (without AWGN), the received signal, in the time domain, can be described by equation (3). Particularizing this formula for a flat channel, one obtains:

$$y[n] = h_0\, x[n - d_0], \tag{13}$$

where h_0 is the complex tap gain and d_0 the corresponding path delay. If one further particularizes for the case where there is no path delay, $d_0 = 0$, and now recalling equation (4), one can write, in the frequency domain:

$$Y_{postFFT}[k] = H_0\, X[k], \qquad H_0 = h_0, \tag{14}$$

which means that not only the channel coefficients are the same for all subcarriers, they are also equal to the complex tap gain defined in the time domain. Additionally, a memoryless block fading channel is being considered, as a result the channel coefficient remains unchanged during one TTI, after which a new uncorrelated coefficient is generated for the next TTI. In turn, since the amplitude of the coefficients has to follow a Rayleigh distribution, $|h_0| \sim R$, and the expected value of its squared amplitude was considered as being equal to one, $E[|h_0|^2] = 1$, the coefficients are drawn from a standard complex normal distribution, $h_0 \sim \mathcal{CN}(0,\ 1)$. It should be noted that two links are being modelled which naturally requires the generation of two independent channel coefficients (h_M and h_B) per TTI.

On the other hand, in order to model the received signal, the expected SNR of both links, $E[SNR_M]$ and $E[SNR_B]$, is set *a priori*. Bearing in mind that MTD and BS are modelled by the same transmitter model (which generates OFDM symbols of average unit power), arises thus the need to adjust their transmit power accordingly. This results in the following signal in the time domain:

$$y = \sqrt{P_M}\, h_M x_M + \sqrt{P_B} h_B\, x_B + \alpha\, w, \tag{15}$$

where P_M and P_B are the average transmit powers, w is the AWGN such that $w \sim \mathcal{CN}(0,1)$ and $\alpha = \sqrt{N_{fft}/N_{tot}}$ is a scaling parameter whose purpose is to guarantee that SNR_M and SNR_B refer to the SNRs after detection (post-FFT) at the receiver as this allows direct comparisons to theoretic results [24]. On a side note, since noise power is defined as being one, the expected SNRs, $E[SNR_M]$ and $[SNR_B]$, are numerically equal to the corresponding average transmit powers, P_M and P_B.

3.3.2.3. Transmitter Model

3.3.2.3.1. Characterization

As previously described, the transmit entities are the MTD and BS, both of which are modelled as two separate LTE downlink transmitters whose model is shown in Figure 10. Notice that the signal processing chain was already described in subsection 2.1.2.2. It is however worth mentioning that, during the scrambling operation, different scrambling sequences are generated according to the physical level identity that is assigned to MTD and BS. Additionally, overheads regarding the pilot signals are not included.

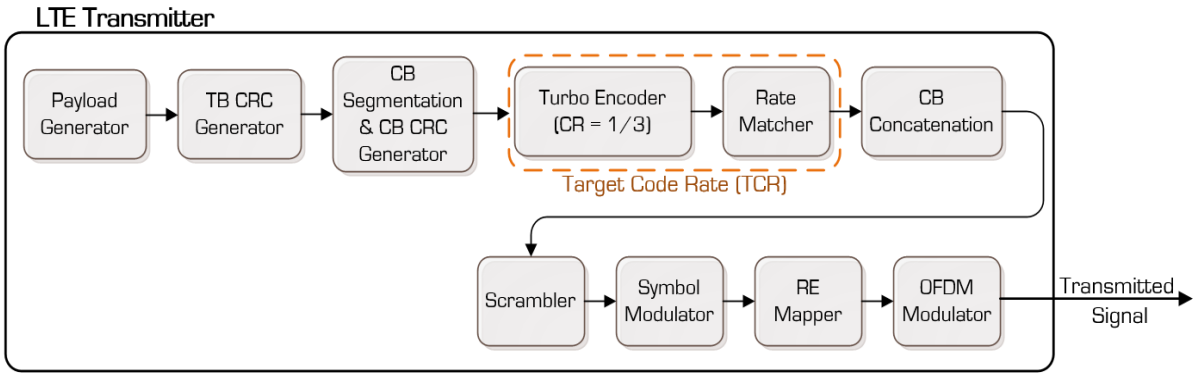

FIGURE 10. BLOCK DIAGRAM OF THE LTE DOWNLINK TRANSMITTER

3.3.2.3.2. Supported Modulation and Coding Schemes

The supported MCSs are shown in Table 3 and are the same as the ones used in [25]. It should be noted that in a real LTE system, the CQI is a 4-bit index, only allowing to report up to 15 different MCSs [12]. Therefore, in such system, the transmitter (BS) uses the CQI report allied to other factors, such as ACK/NACK rate, to determine the MCS. In this work, the author considered that the CQI is not restricted to 4 bits such that the receiver is able to report any of the available schemes. The MCS selection, for the I2D link, is thus delegated to the receiver. On the other hand, the D2D link uses a fixed MCS corresponding to CQI 1 and as such there is no need to report the CQI since LA is not performed.

TABLE 3. CQI-TO-MCS LOOK-UP TABLE

CQI	Modulation	Code Rate
1	4-QAM	1/9
2	4-QAM	1/6
3	4-QAM	0.21
4	4-QAM	1/4
5	4-QAM	1/3
6	4-QAM	0.42
7	4-QAM	1/2
8	4-QAM	0.58
9	4-QAM	2/3
10	4-QAM	0.73
11	16-QAM	0.43
12	16-QAM	0.46
13	16-QAM	1/2
14	16-QAM	0.54
15	16-QAM	0.58
16	16-QAM	0.61
17	64-QAM	2/3
18	64-QAM	0.73
19	64-QAM	4/5
20	64-QAM	0.58
21	64-QAM	0.62
22	64-QAM	2/3
23	64-QAM	0.70
24	64-QAM	0.74
25	64-QAM	4/5
26	64-QAM	0.85
27	64-QAM	0.90

3.3.2.4. Receiver Model

3.3.2.4.1. Characterization

As discussed in subsection 2.1.3.2.2, there are two types of SIC strategies that are applicable to LTE. Rather than applying Soft SIC, the implemented receiver follows a Hard SIC strategy. It is known that Hard SIC does not perform as good as Soft SIC, but, given the context of this work whose main purpose is to evaluate different LA strategies under the cellular downlink with low-fixed-rate D2D underlay, adopting a Hard SIC strategy does not compromise this objective, with the added benefit of being significantly less computationally intensive and thus allowing simulations to run faster. That said, the implemented receiver can be described as a Hard SIC receiver based on TB CRC checks.

In the literature, namely where SIC is applied to LTE systems, the focus is on cancelling transmissions from multiple antennas, MIMO transmission, pertaining to the same transmit entity [19], [26]. In such case, all the signals share the same MCS, it thus follows that the optimal order of decoding is to sort the signals according to their SINR such that the signal experiencing the highest SINR is decoded first. In the case that is being studied, this does not apply, as MTD and BS generally encode their messages with different MCSs. Consequently, the rule to determine the order of decoding is not based on which link experiences the highest SINR, but rather on how great the margin between the experienced SINR and the threshold associated to the given MCS is. Let $\mathrm{SINR}_{\mathrm{M}}$ and $\mathrm{SINR}_{\mathrm{B}}$ be the post-detection instantaneous SINR of the D2D and I2D links respectively, while Γ_{M} and Γ_{B} are the thresholds associated to $\mathrm{MCS}_{\mathrm{M}}$ and $\mathrm{MCS}_{\mathrm{B}}$. The implemented ordering and SIC process can then be described as follows:

1. $\Gamma_M = \text{get\_threshold}(\text{MCS}_\text{M})$ // fixed MTD MCS – known *a priori*
2. **for** new $\text{SINR}_\text{M}, \text{SINR}_\text{B}$ **do** // new channel conditions (I2D)
3. $\Gamma_B = \text{get\_threshold}(\text{MCS}_\text{B})$
4. **if** $\text{SINR}_\text{M} - \Gamma_\text{M} \geq \text{SINR}_\text{B} - \Gamma_\text{B}$ **then** // determine the decode order
5. $s_1 = \text{M}; s_2 = \text{B};$
6. **else**
7. $s_1 = \text{B}; s_2 = \text{M};$
8. **end if**
9. $\text{decode}(s_1)$
10. **if** $\text{TB\_CRC\_check} == \text{true}$ **then**
11. $\text{cancel}(s_1); \text{decode}(s_2);$
12. **else**
13. $\text{decode}(s_2)$
14. **if** $\text{TB\_CRC\_check} == \text{true}$ **then**
15. $\text{cancel}(s_2); \text{decode}(s_1);$
16. **end if**
17. **end if**
18. **end for**

FIGURE 11. IMPLEMENTED SIC ALGORITHM

Notice that, in order to obtain smooth performance curves, even if the margins are negative the implemented receiver still attempts to decode. Similarly, if the receiver cannot decode the signal that has been determined to be the first, it still attempts to decode the other signal. If successful, cancels the contribution of the latter and re-attempts to decode the former.

The receiver model is shown in Figure 12 and it can be observed that to perform IC, there is the need to re-encode the decoded message to obtain the transmitted QAM symbols. Additionally, the UE has perfect knowledge of both CSIs and, as such, rather than estimating the CSIs based on reference signals, genie information is used instead.

Another aspect worth mentioning is the equalization process. The implemented receiver applies ZF (Zero-forcing) frequency-domain equalization such that the weight to be applied to each received symbol is

$$w = \frac{1}{\sqrt{P_D}\, h_d}, \qquad \textbf{(16)}$$

where P_D is the average transmitted power of the signal to be decoded and h_d the corresponding complex channel gain. Recall that the channel is block flat, thus h_d is the same for all the detected symbols within one TTI.

After equalization, the bit LLRs (Log-Likelihood Ratios) are generated by the soft symbol demodulator, based on a soft sphere algorithm [22], [27], [24]. All the other unspecified functional blocks correspond to the dual operations of those performed at the transmitter and the only noteworthy aspect is that for the Turbo decoder an 8-iteration max-log-MAP algorithm was chosen.

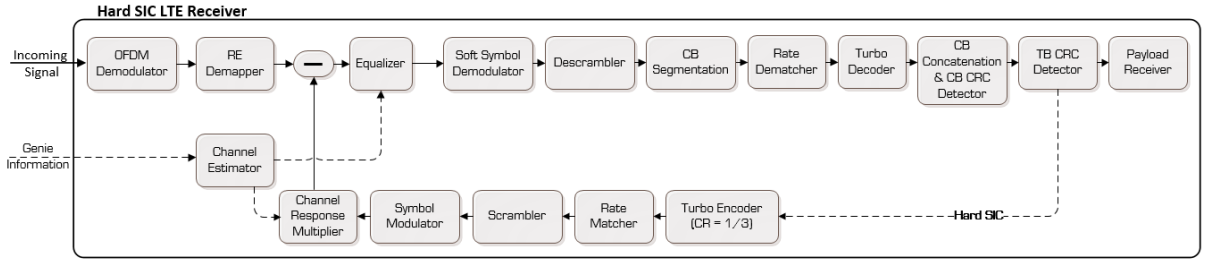

FIGURE 12. BLOCK DIAGRAM OF THE IMPLEMENTED LTE RECEIVER

3.3.2.4.2. SINR-to-CQI mapping

As previously mentioned, link adaptation is designed to dynamically assign a suitable CQI to match the channel conditions. In order to achieve this, the receiver determines the effective SINR and chooses the CQI based on a look-up table whose results were obtained from a SISO AWGN simulation for each MCS such that a BLER lower than 10% is achieved. These results are shown in Figure 13 and Figure 14**.**

In frequency-selective fading channels, distinct subcarriers generally experience different SINRs and, as a result, there is a need to calculate an effective SINR based on a compression method (MIESM or EESM) [13] [16] such that there is a close match between the BLERs of the equivalent AWGN channel and the real fading channel. However, in a block flat fading channel, all subcarriers

experience the same SINR conditions within a TTI and, as such, this calibration step can be avoided since its performance for a given SINR is similar to that of the AWGN.

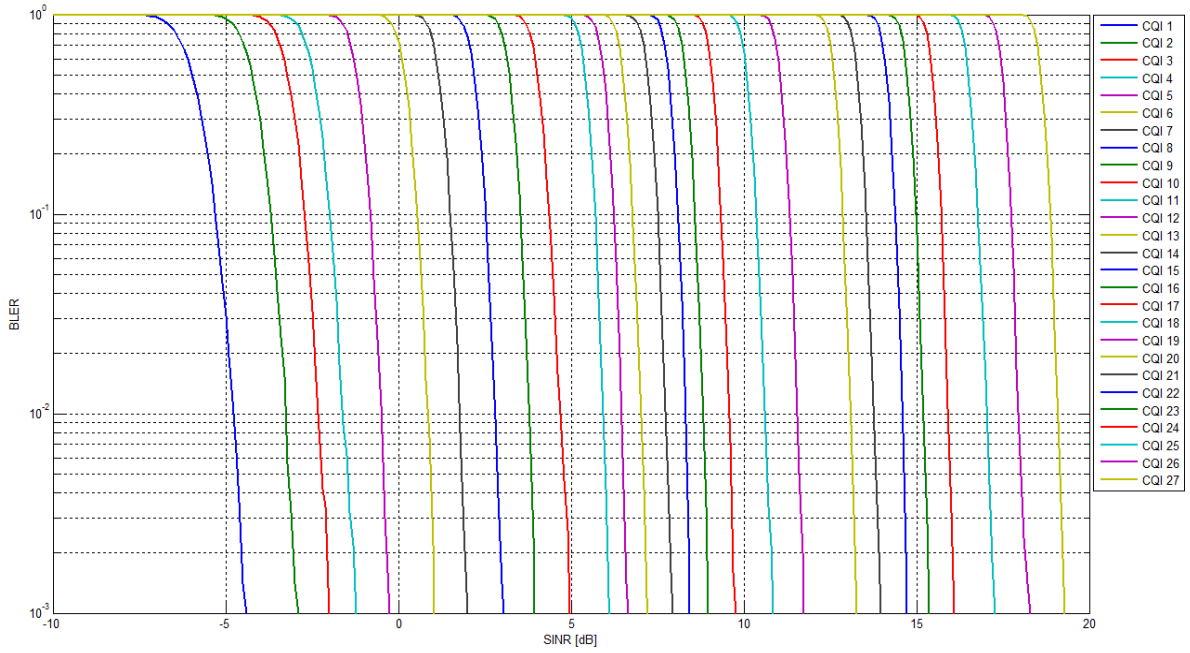

FIGURE 13. BLER AWGN CHANNEL

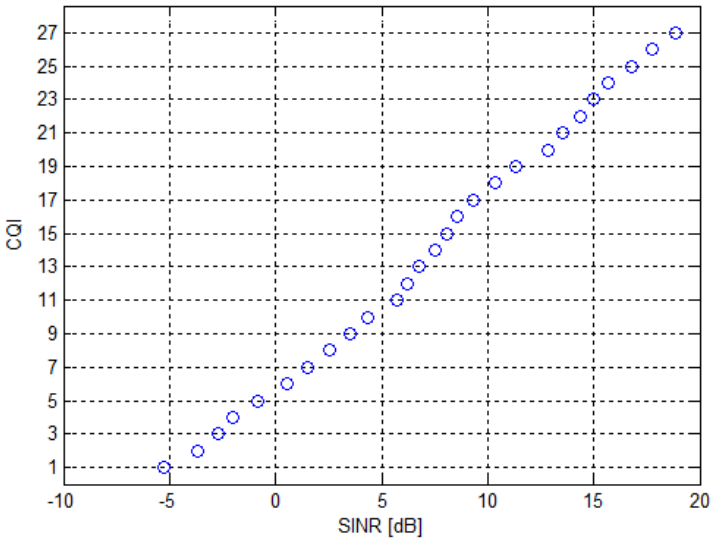

FIGURE 14. SINR-TO-CQI MAPPING (10% BLER)

Additionally, it should be noted that if a link experiences a SINR below the threshold of the lowest CQI (CQI 1), then the target BLER will increase. On the other hand, for a SINR above the threshold of the highest CQI (CQI 27), the BLER will be lower. It is also noteworthy that even if the SINRs fall within the range depicted in Figure 14, it is expected that the BLER will be substantially lower than 10%

because, despite having 27 schemes, the spacing is roughly 1dB and, from Figure 13, it can be seen that there is a sharp decrease in BLER with SINR.

3.3.2.5. Operation Modes

In this study, four different operation modes were considered and are the following:

1. Orthogonal mode: D2D and I2D links occur simultaneously, but different resources are assigned to each link. There is thus no interference, at the expense of having to allocate twice the bandwidth. The strategy to adapt the I2D link is based on the received instantaneous SNR (SNR_B).

2. Legacy mode: D2D and I2D links occur simultaneously and share the same resources which leads to interference. However, the receiver (UE) is not capable of performing SIC. It then follows that the strategy used to adapt the I2D link is based on the received instantaneous SINR ($SINR_B$).

3. SIC mode with zero-outage rule: Similar to the previous mode, both links operate at the same time and share the same resources. The UE is now a SIC-capable device and the LA strategy follows the zero-outage rule described in subsection 2.1.4.2.

4. SIC mode with weighted rule: Same conditions as the previous mode, except that the adopted LA strategy is based on the weighted rule whose description can be found in subsection 2.1.4.3.

It is now clear that the last two operation modes are the proposed modes, while the other two only serve as a benchmark.

3.3.3. System Level Model

In order to evaluate the operation modes previously described under the system level scenario (see subsection 3.2.2.2), the simulator first determines the position of the receiver. Then the path losses of the D2D and I2D links are computed (A_M and A_B). The former is fixed, but the latter depends on the position of the receiver. Thus, there is the need to determine the I2D path loss map. For this purpose, the MATLAB script provided by METIS was used [28].

The formulas which allow $E[SNR_M]$ and $E[SNR_B]$ to be determined are (in dB):

$$E[SNR_i] = P_{TX_i} + G_i - A_i - NF_U - \sigma_w^2, \;\; i \in \{M, B\} \quad \textbf{(17)}$$

$$\sigma_w^2 = N_0 + 10\log_{10}(BW_T). \quad \textbf{(18)}$$

After determining the pair $(E[SNR_M], E[SNR_B])$ pertaining to a given position, the corresponding set of values $(BLER_M, Throughput_M, BLER_B, Throughput_B)$ are obtained by using the results presented in subsection 4.2. It is worth mentioning at this point that the link level results were obtained with steps of $1dB$. Since the pair $(E[SNR_M], E[SNR_B]) \in \mathbb{R}^2$, linear interpolation was used. Additionally, in the link level simulations $-20 \leq E[SNR] \leq 80\ [dB]$, therefore if the pair $(E[SNR_M], E[SNR_B])$ takes values outside the range, the bound values are applied instead.

The simulation parameters used are presented in Table 4 [21], [29], [30].

TABLE 4. SYSTEM LEVEL SIMULATION PARAMETERS

Environment						
Building Layout	**No.**	**Floors**	**Floor Height [m]**	**Length x Width [m]**		**Spacing [m]**
	4	8	3.5m	120x120		18
Network Layout	**BS height [m]**	**UE Height [m]**	**Trials**			
	3.5 (roof #2)	1.5	500 per floor (building #3)			
Network						
Both Links	**Carrier Freq. [MHz]**	**Transmission Bandwidth (BW_T)[MHz]**	**Noise Spectral Density (N_O)[dBm/Hz]**	**UE Noise Figure (NF_U) [dB]**	**UE Antenna Gain [dBi]**	**Traffic Model**
	800	1.08	-174	9	0	Full Buffer
I2D Link	**BS TX Power (P_{TX_B}) [dBm]**	**BS Antenna Gain after cable loss (G_B)[dBi]**		**Small-scale Fading (Link Level)**	**MCL [dB]**	**Propagation Model**
	46	15		Block Flat Rayleigh	70	PS#4 (Macro O2I)
D2D Link	**MTD TX Power (P_{TX_M})[[dBm]**	**MTD Antenna Gain (G_M)[[dBi]**		**Small-scale Fading (Link Level)**	**MCL [dB]**	**Propagation Model**
	0	0		Block Flat Rayleigh	60	MCL is assumed

Chapter 4. Results and Discussion

4.1. Introduction

In this chapter, the results from the simulations specified in the previous section are presented and analyzed.

The author focuses first on the link level simulations as they serve as basis to develop the system level simulations, while also giving a more broad understanding of the behavior of the different operation modes that were specified in subsection 3.3.2.5. The system level results are presented and discussed at the end of the chapter.

4.2. Link Level Simulations

4.2.1. Introduction

In this subchapter, the operation modes are evaluated in respect to the individual BLER, throughput rate per total number of RBs assigned (to both links) and combined spectral efficiency (ε) which is defined as the product of the absolute throughput of I2D (R_B) and D2D (R_M) links normalized to the total allocated bandwidth (B_W):

$$\varepsilon = \frac{R_B R_M}{BW}. \quad \textbf{(19)}$$

As a complementary note, the product is used in preference to the sum of the throughputs as the D2D link can only achieve a fraction of the throughput of the I2D link due to the usage of a low MCS by the former. Hence, by performing the multiplication, not only the metric treats the links in a fairer fashion, but also makes it easier to pinpoint the regions where both links are simultaneously operating at relatively high throughput.

4.2.2. Average MCS

In Figure 15, the average MCS used by the I2D link is shown. Recall that while the BS is allowed to dynamically change its MCS, the MTD encodes its messages with a fixed MCS corresponding to what has been previously defined as CQI 1 (see subsection 3.3.2.3.2).

As a general rule, the higher the $E[SNR_B]$, the higher the average MCS is, being the legacy mode the exception unless low values of $E[SNR_M]$ (hence, high $E[SINR_B]$) are involved.

Comparing the SIC modes, it can be observed that mode 3 chooses more robust MCSs so much so that the highest MCS used is 10, while mode 4 uses the full range of MCSs.

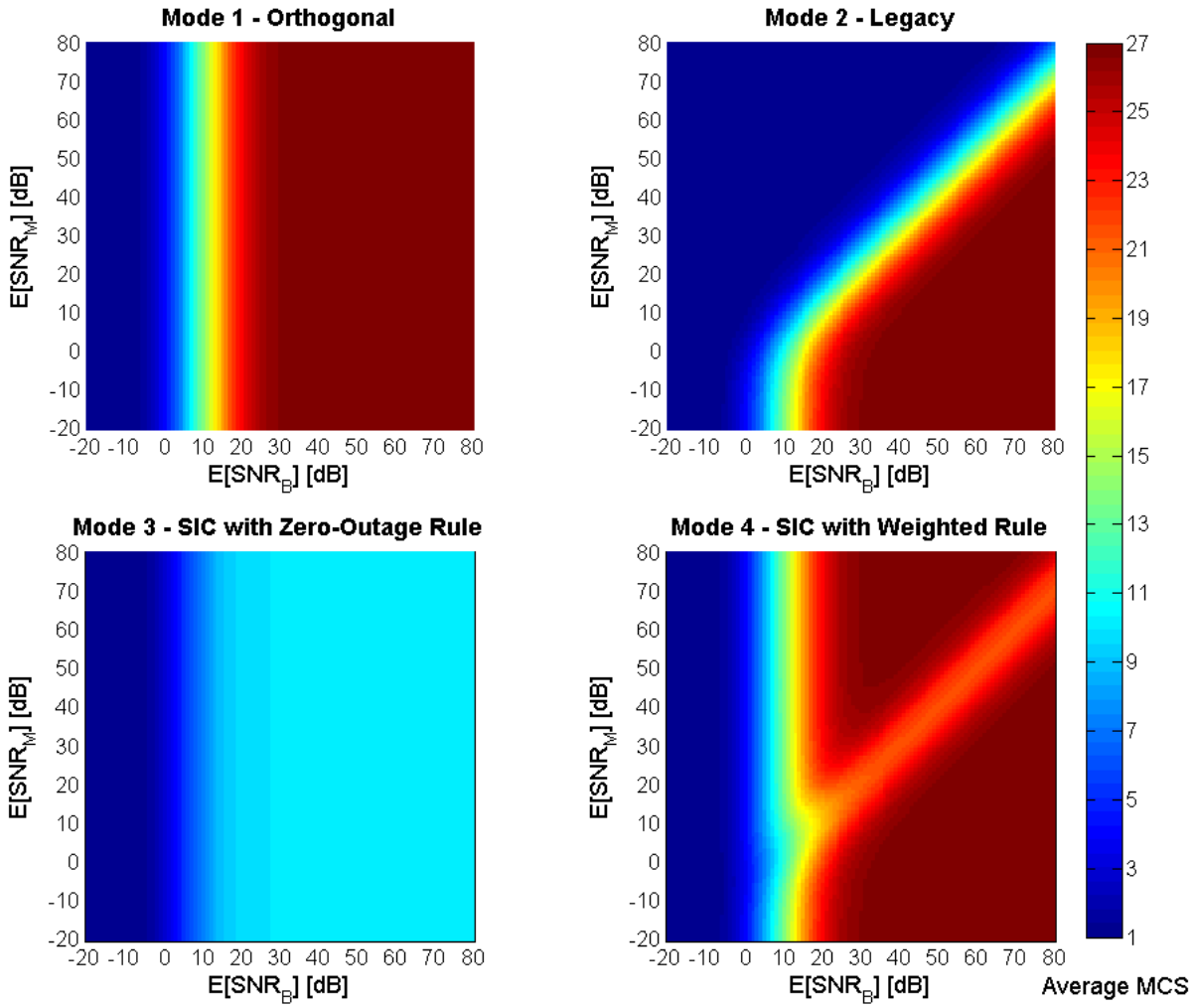

FIGURE 15. I2D AVERAGE MCS

4.2.3. BLER

Overall, the D2D link is less prone to errors which can readily be observed by comparing the BLER of both links (Figure 16 and Figure 17) for any given method under reversed $E[SNR]$ conditions. This is consistent with the expected behavior because the I2D link has an average CQI that is higher (hence, a less reliable average MCS) than the one used in the D2D link.

Another general observation is that, in the operation modes where both links share the same resources (all except the first), similar $E[SNR]$ conditions in both links lead to a higher BLER because, on average, there is not a strong signal that can be easily detected and cancelled according to the SIC algorithm. In a system where both links have the same MCS, the system would exhibit the worst performance when the received signals of both links have similar SNR (SIR near 0 dB). However, this does not happen because the BS uses, overall, a higher MCS than the MTD. Consequently, this worst

performance region is slightly shifted and it will happen when $E[SNR_B]$ is higher than $E[SNR_M]$. Another consequence is that higher $E[SNR]$ values do not necessarily mean lower BLERs as observed in the regions where $E[SNR_M]$ and $E[SNR_B]$ are both high (modes 2 and 4).

Continuing with the analysis, from all the operation modes, orthogonal mode (mode 1) achieves the best performance while the legacy mode (mode 2) the worst. This result is intuitive because, in mode 1, D2D and I2D signals do not interfere with one another, while, in mode 2, they do. And since the latter does not perform any kind of cancellation (unlike modes 3 and 4), it is natural that, when the interference has a significantly higher strength, the receiver is less likely to be able to decode the intended signal successfully. Additionally, it should be noted that modes 3 and 4 exhibit a performance that is similar to that of mode 1 if only the region where $BLER > 10^{-2}$ is to be considered.

Another noteworthy observation is that, in the region that has been previously described as SIC worst performance region (SIR close to 0 dB), mode 3 achieves a lower BLER than modes 4 which is explained by the fact that, on average, base station uses a more robust MCS.

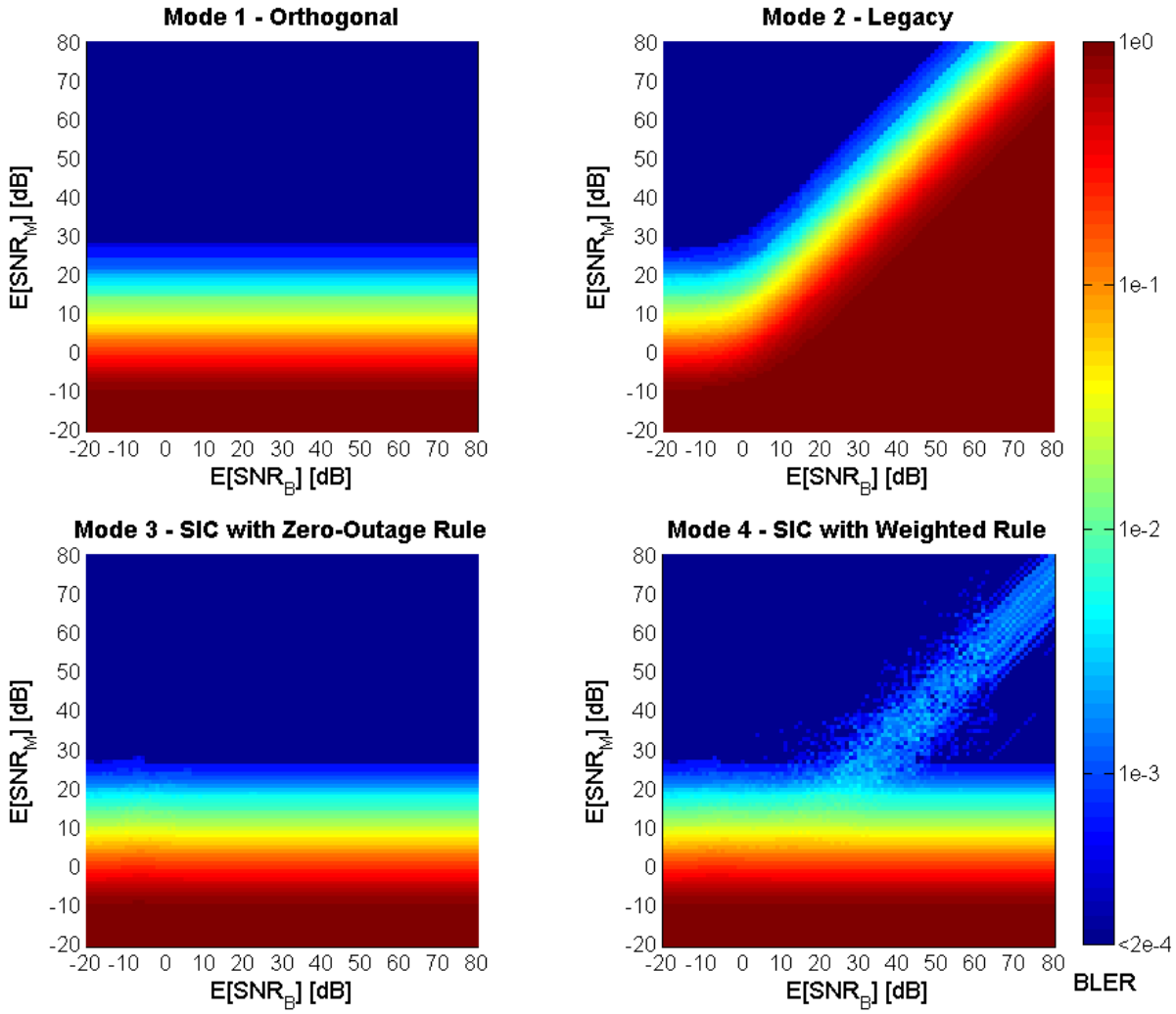

FIGURE 16. D2D BLER

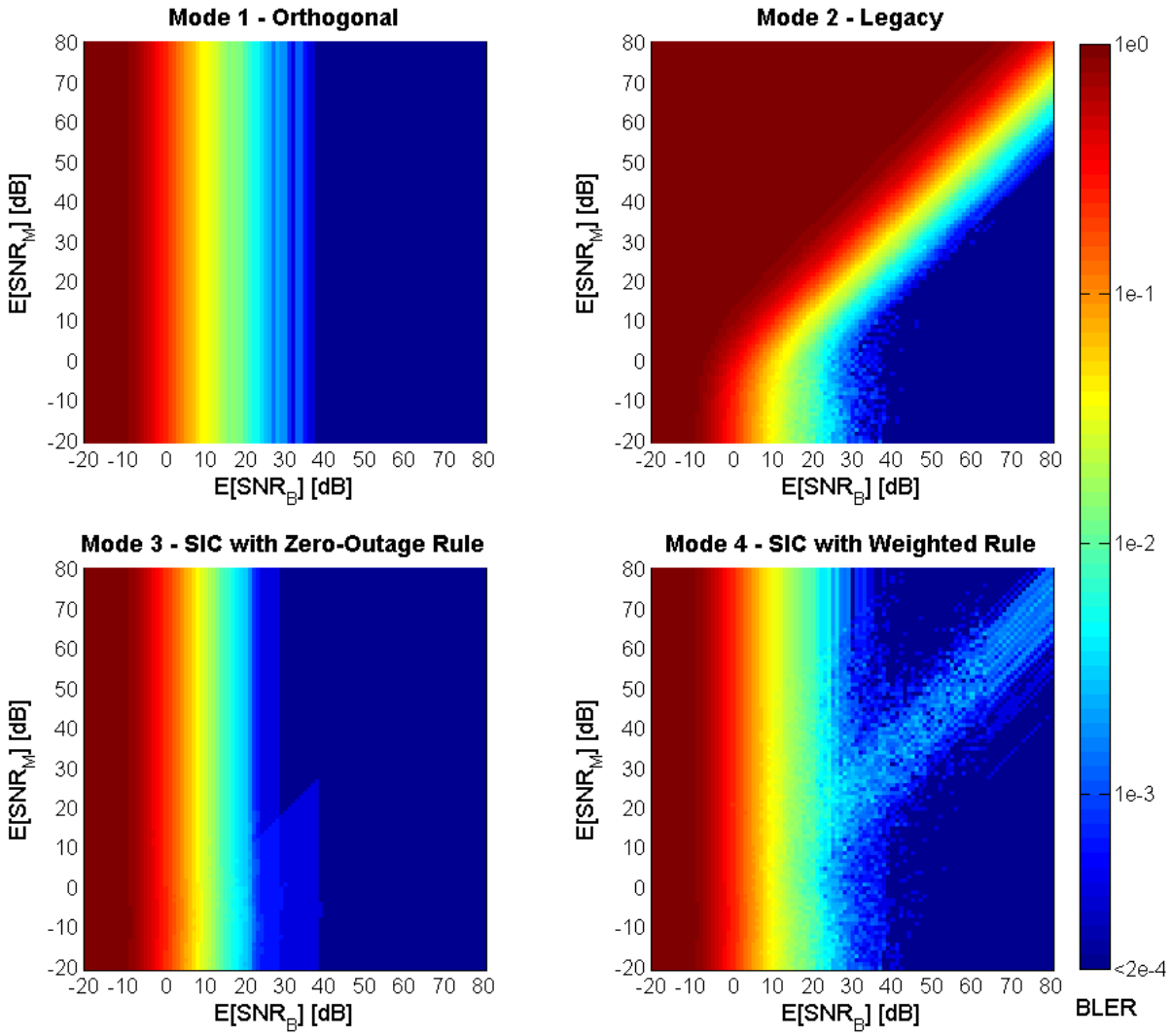

FIGURE 17. I2D BLER

4.2.4. Throughput Rate per total RBs used

Regarding the D2D throughput, in Figure 18, it can be observed that it is proportional to the success probability ($1 - BLER$) given that the MTD always uses the same MCS. Additionally, its throughput does not change significantly once its $BLER < 10^{-2}$, so, from a throughput standpoint, there is barely no gain in trying to achieve a lower D2D BLER. That said, modes 1, 3 and 4 exhibit similar behavior (absolute throughput), but the SIC modes are twice as efficient because they require half the RBs.

Moving on to the I2D throughput, whose results are shown in Figure 19, it is readily seen that overall a lower I2D BLER leads to a higher throughput for a given mode. However, since the BS has the capability of adapting its MCS and chooses it differently across different modes, it follows that, despite the fact that the zero-outage rule achieves a lower BLER, it does not reach a throughput as high as the weighted rule. This occurs because the loss of efficiency inherent to using a significantly more conservative MCS outweighs the gain in having a lower BLER which results in an inferior throughput. From all modes, weighted rule achieves the best performance as it is able to switch between different metrics in order to choose the MCS that is likely to perform the best given the conditions of both links.

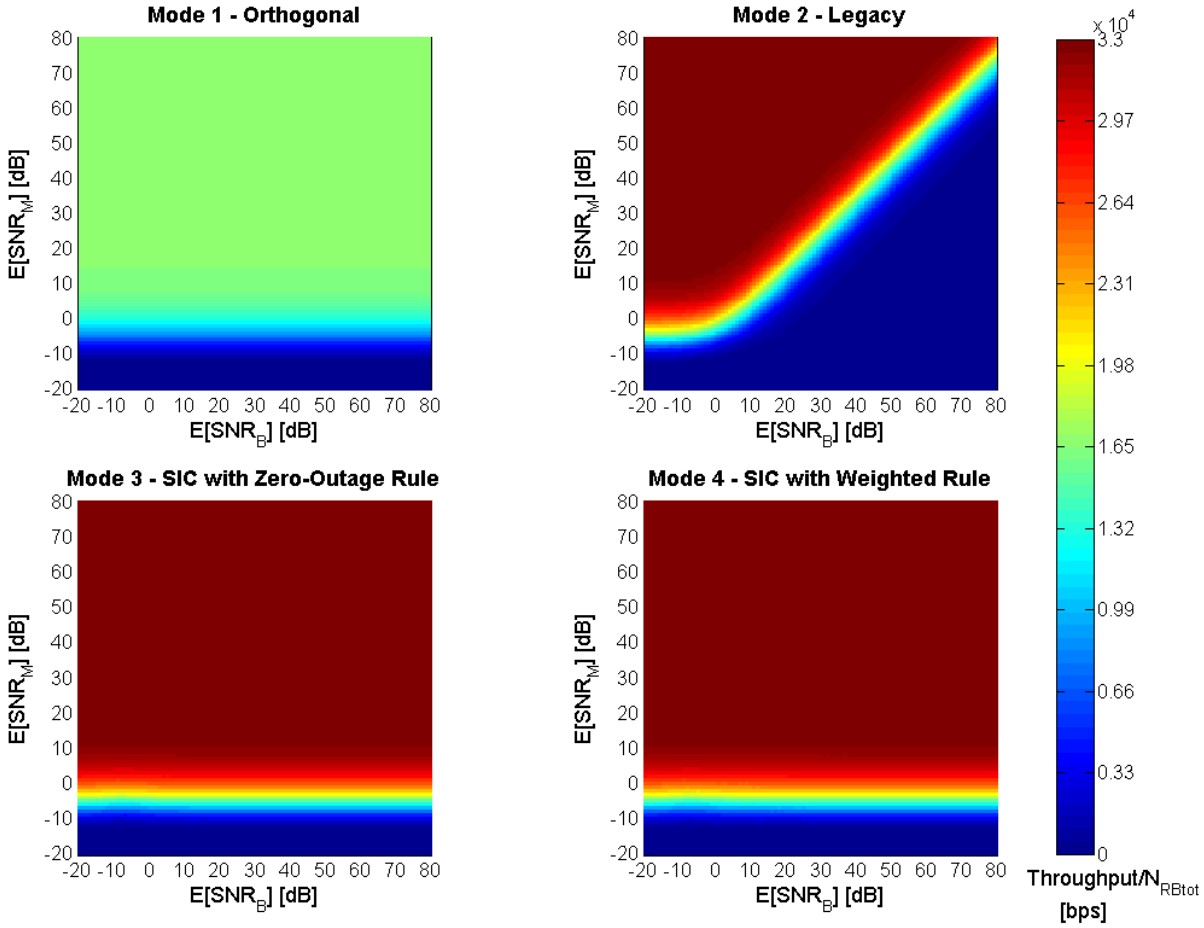

FIGURE 18. D2D THROUGHPUT PER TOTAL RBS USED

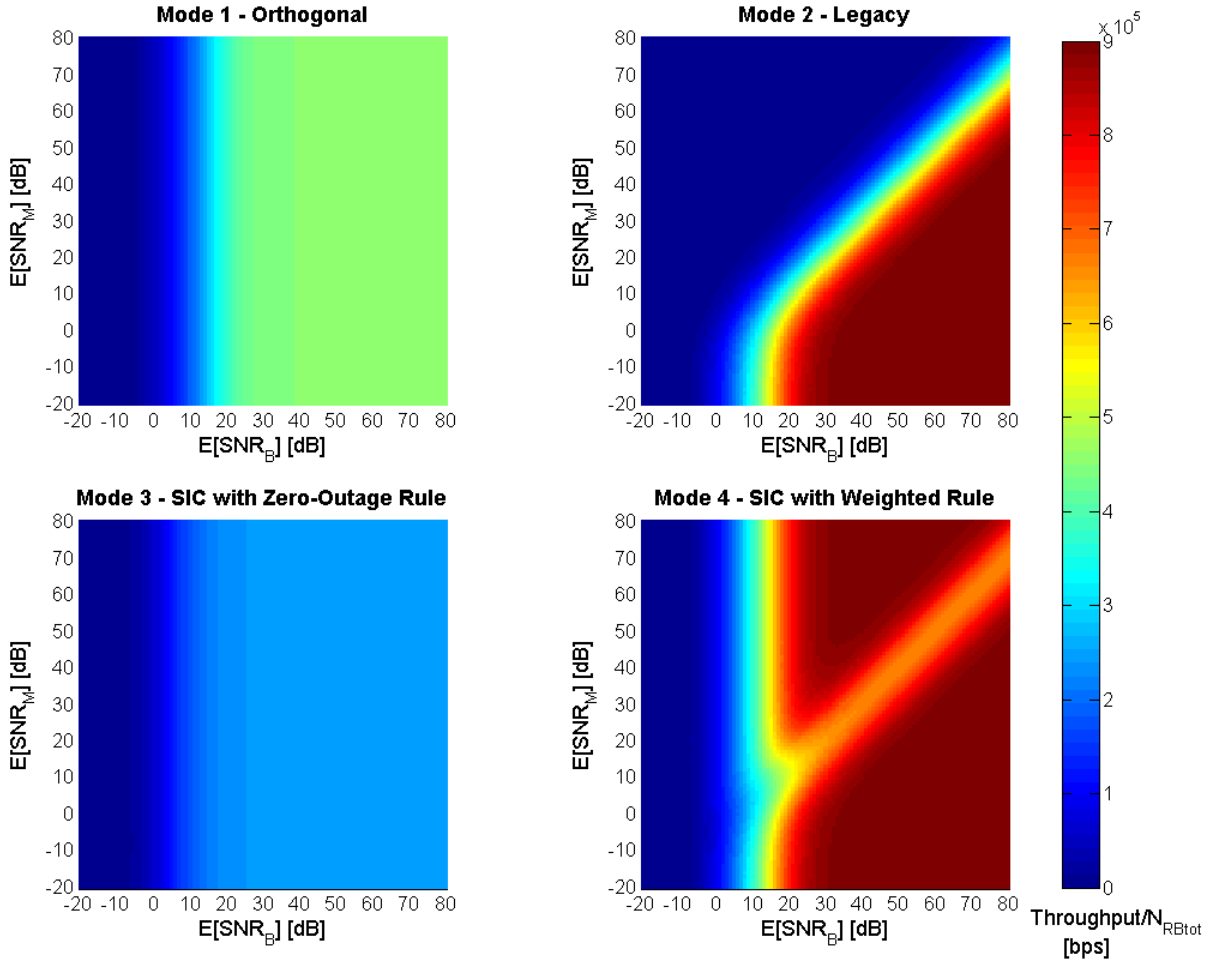

FIGURE 19. I2D THROUGHPUT PER TOTAL RBS USED

4.2.5. Combined Spectral Efficiency

The fact that the SIC mode with weighted rule provides the best performance is further highlighted in the combined efficiency plots shown in Figure 20. It can achieve an efficiency that is always equal or higher than any other modes including the orthogonal mode. It can be twice as efficient as the latter and up to four times as efficient as the SIC mode with zero-outage rule.

According to this metric, it is clear that, from all modes, legacy has the worst performance as it cannot achieve high throughputs in both links simultaneously.

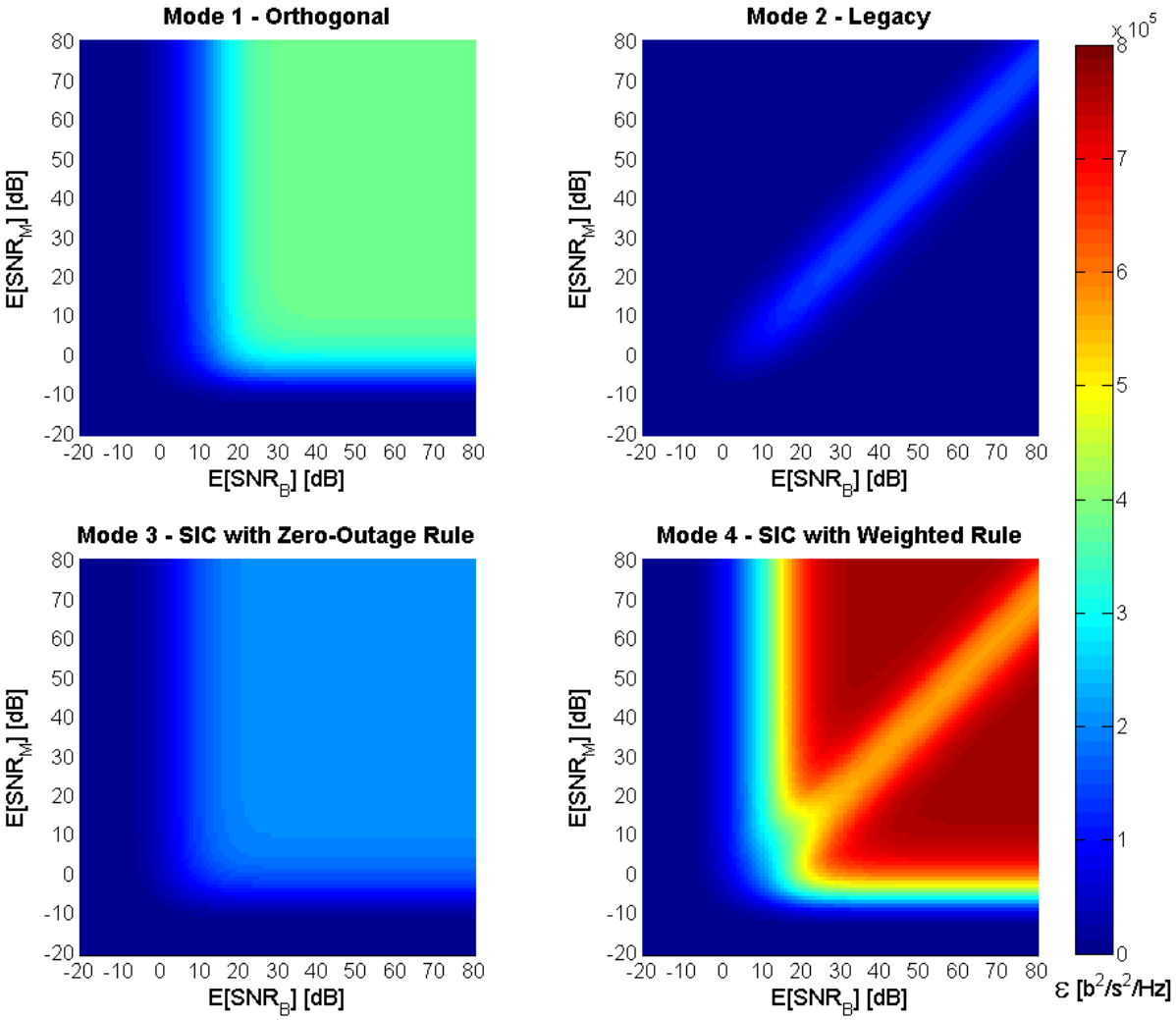

FIGURE 20. COMBINED SPECTRAL EFFICIENCY

4.3. System Level Simulations

4.3.1. Introduction

In this subchapter, the results corresponding to the system level model described in subsection 3.3.3 are presented. This subchapter is divided into two parts: intermediate and final results. The intermediate results shown are the path losses and the CDFs (Cumulative Density Functions) of the estimated D2D and I2D SNRs. The latter allows then to compute the final results, namely the metrics whose purpose is to evaluate the various operation modes under the system level scenario (indoor on-body MTD).

4.3.2. Intermediate Results

4.3.2.1. Path Losses

Figure 21 shows the computed losses that the BS signal experiences across the 8 floors. Note that only the building 3 (south-west building) is of interest. As expected, the losses are higher in the south-west corner of each floor and on the bottom of the building due to a greater travel distance.

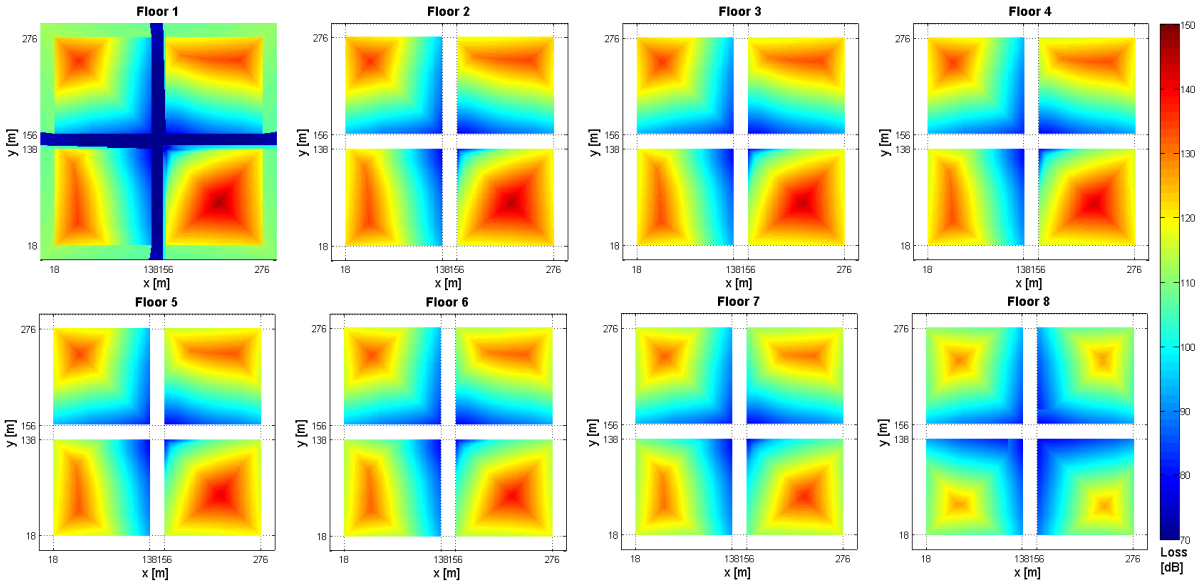

FIGURE 21. I2D PATH LOSS MAP

Recall from subsection 3.3.3 that the D2D path loss is fixed and is equal to 60dB.

4.3.2.2. CDF of expected SNR

Figure 22 shows the CDF of the expected SNR experienced by the I2D link and further proves that when the user is located in the lower floors lower $E[SNR_B]$ are more likely to occur. It should be noted that since the D2D path loss is always the same, $E[SNR_M]$ is also fixed for all instances. Plugging the parameters described in subsection 3.3.3, one obtains $E[SNR_M] \approx 44.67dB$.

In order to analyze the behavior of the various operation modes in a more intuitive fashion, the CDF of $E[SINR_B]$ and $E[SINR_M]$ were also computed and are shown in Annex A. It is apparent from equation (12) that calculating the exact $E[SINR]$ requires the knowledge of the instantaneous SNRs rather than the $E[SINR]$ values. In fact, plugging the $E[SNR]$ instead, results in the lower bound (see Annex B). Thus, in order to get a better estimate of $E[SINR]$, equation (26) derived in Annex C was used.

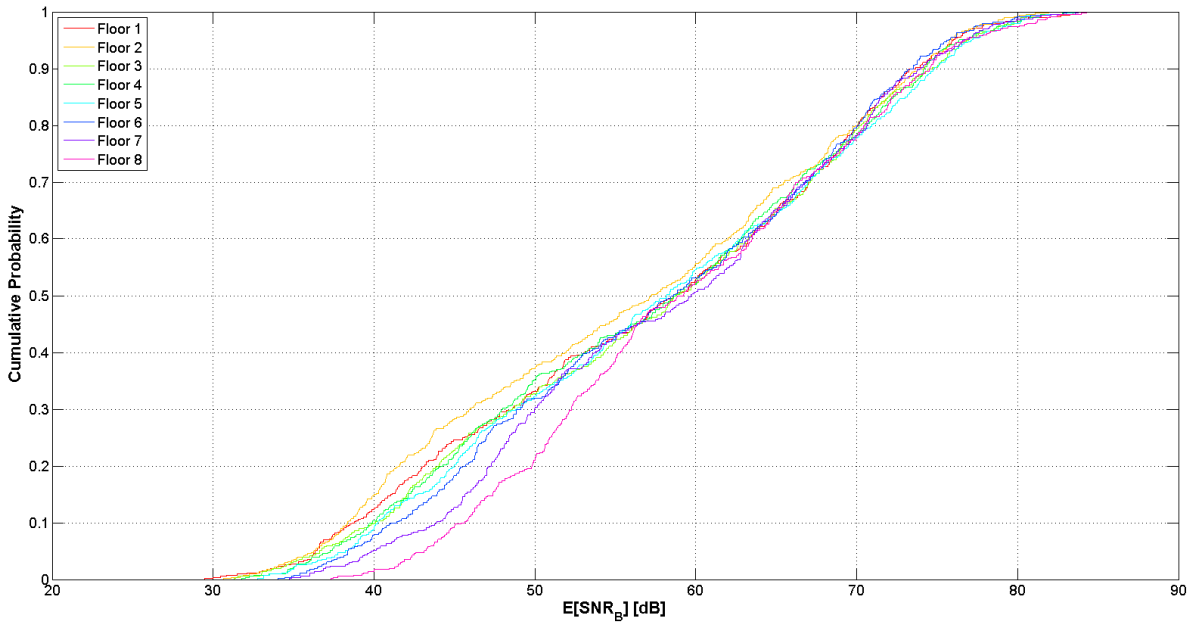

FIGURE 22. CDF OF EXPECTED I2D SNR

4.3.3. Final Results

4.3.3.1. CDF of I2D Average MCS

The plots corresponding to the average MCS used in the I2D link are shown in Figure 23.

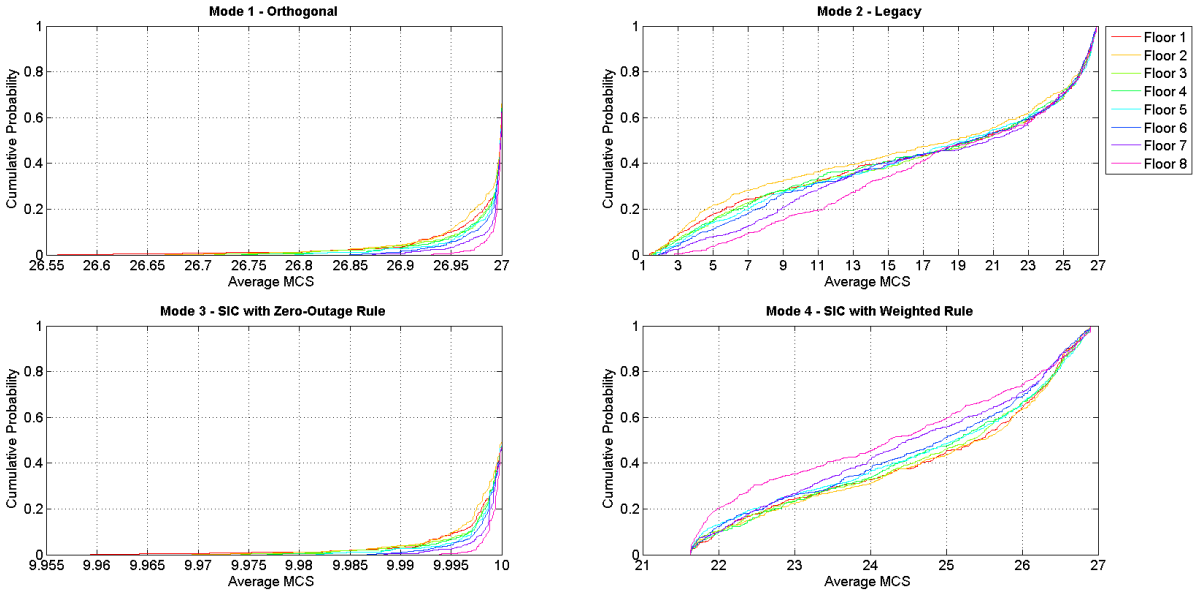

FIGURE 23. CDF OF I2D AVERAGE MCS

In the orthogonal mode, since the D2D link does not cause any interference, the I2D average MCS corresponds to the highest across virtually all floors which is explained by the fact that I2D link operates almost exclusively in the high SNR regime regardless of the floor where the user is, thus leading to very small fluctuations. In the legacy mode, however, the D2D and I2D links share the same resources, thus rather than choosing the MCS according to SNR_B, $SINR_B$ is used instead. Observing the CDF of $E[SINR_B]$, in Annex A, it is natural that the average chosen MCS is significantly different depending on the position of the user.

In the SIC mode with zero-outage rule, despite the interference caused by the D2D link, the I2D link uses a similar MCS regardless of the position of the receiver. It is worth noting that the MCS chosen is significantly higher, in the case where the weighted rule is applied which, in turn, meets the design criteria: mode 3 focuses on reliability by using robust MCSs, while mode 4 tries to maximize the throughput.

4.3.3.2. CDF of BLER

In the legacy mode, no cancellation is performed and the messages are decoded independently, therefore the BLER, in comparison to all the other modes, is high for D2D and I2D links (Figure 24 and Figure 25 respectively). A receiver in the higher floors is likely to experience a $SINR_M$ that is below the lowest threshold (roughly -5dB) which results in an increased $BLER_M$. A similar behavior happens for the I2D link, but applied to lower floors.

It should be noted that since the simulation length is 5000 TTIs, the minimum resolution is a BLER of $2 * 10^{-4}$ which, in turn, means that $BLER_M$ is very low for modes 1 and 3. Although not visible, it is expected that mode 1 can achieve a slightly lower $BLER_M$ because, first, no interference occurs and, secondly, the D2D link operates at a fixed (and already at the most robust) MCS, therefore mode 3 cannot perform robust LA to circumvent the existence of interference due to the I2D link. Additionally, the fact that mode 3 uses a SIC-capable receiver, allied to robust LA on the I2D link, leads the author to believe that the performance between the two does not differ significantly in regards to $BLER_M$. On the other hand, comparing their behavior in regards to $BLER_B$, the former can achieve a better performance, mostly due to the fact that mode 3 uses more robust MCSs.

It is also worth mentioning that the SIC mode with weighted rule does not achieve BLERs as low as modes 1 or 3, but shows nonetheless a good performance.

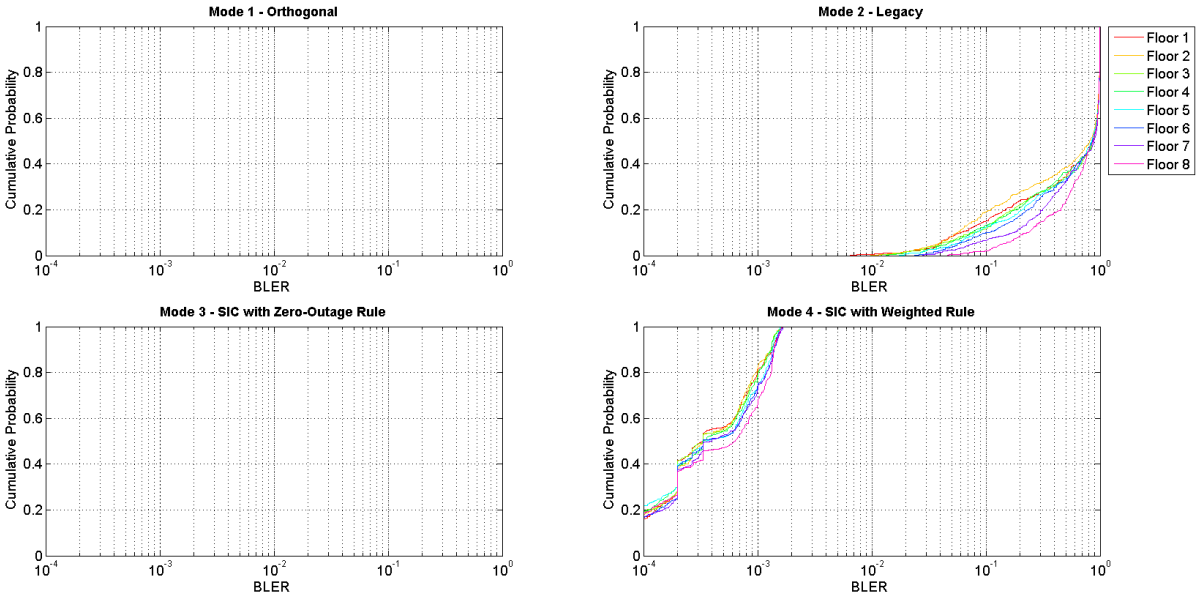

FIGURE 24. CDF OF D2D BLER

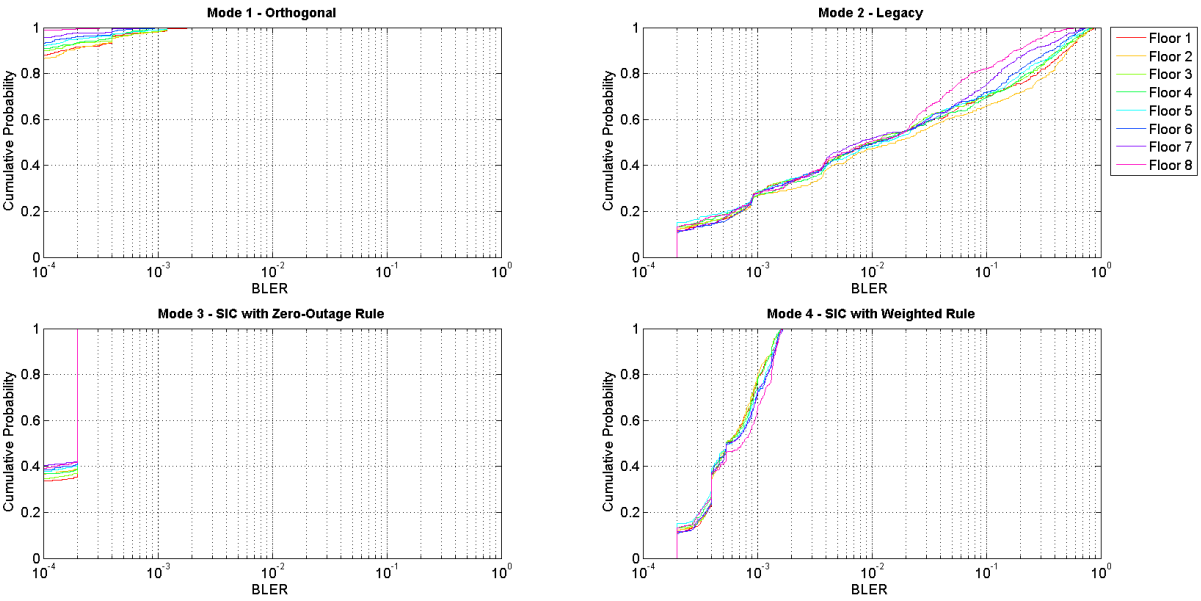

FIGURE 25. CDF OF I2D BLER

4.3.3.3. CDF of Throughput Rate per total RBs used

As already stated, in the D2D link, its throughput (Figure 26) is proportional to its BLER. Naturally, in the legacy mode the user experiences a wide range of throughput rates, while in the orthogonal or SIC with zero-outage rule the throughput is always the maximum. Although achieving the same absolute throughput, in the orthogonal mode, twice the resources are allocated, thus the throughput in the latter is halved. Note that even in the legacy mode, the receiver can experience, albeit not consistently, higher throughput rates than that of orthogonal mode. Both SIC modes experience similar D2D throughputs.

In Figure 27 the throughputs obtained for the I2D link are presented. It is clear that either in the orthogonal mode or SIC with zero-outage rule, the range of throughputs experienced by the receiver is very contained so much so that it is roughly 9kbps and 1kbps respectively. Despite using twice the resources, orthogonal mode reaches a throughput that is almost twice than that of mode 3. On the other hand, legacy mode experiences a range of throughputs that covers the whole range of possible throughputs, while in the SIC with weighted rule the lowest throughput is around 665kbps which is greater than the highest observed in orthogonal mode or SIC with zero-outage rule.

That said, it is no surprise that SIC with weighted rule is the mode that performs the best in regards to throughput.

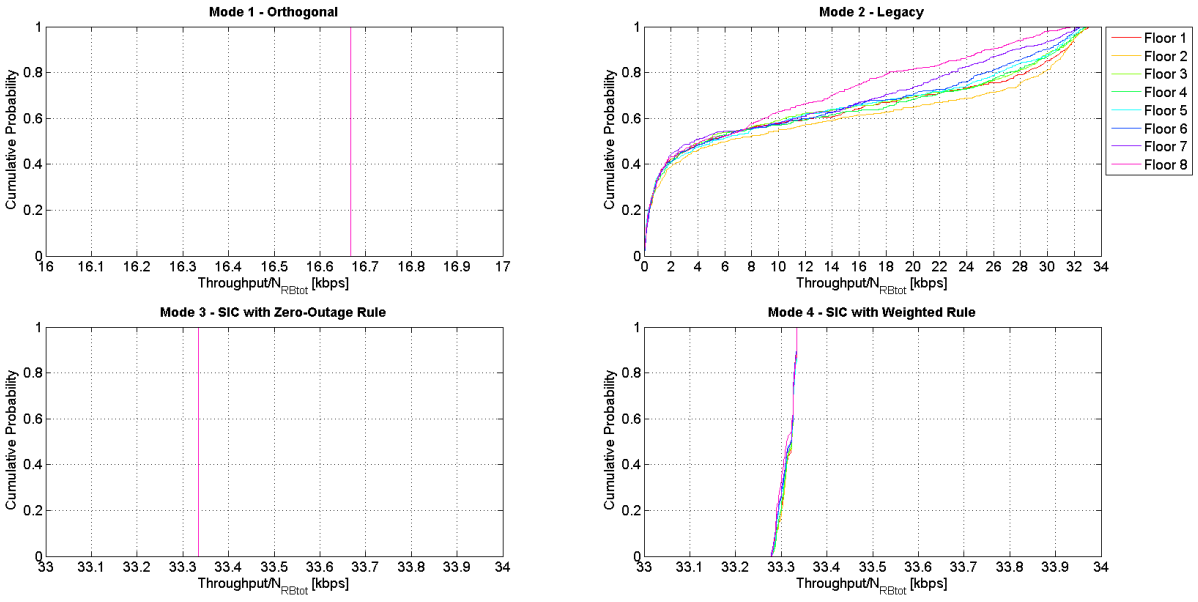

FIGURE 26. CDF OF D2D THROUGHPUT PER TOTAL RBS USED

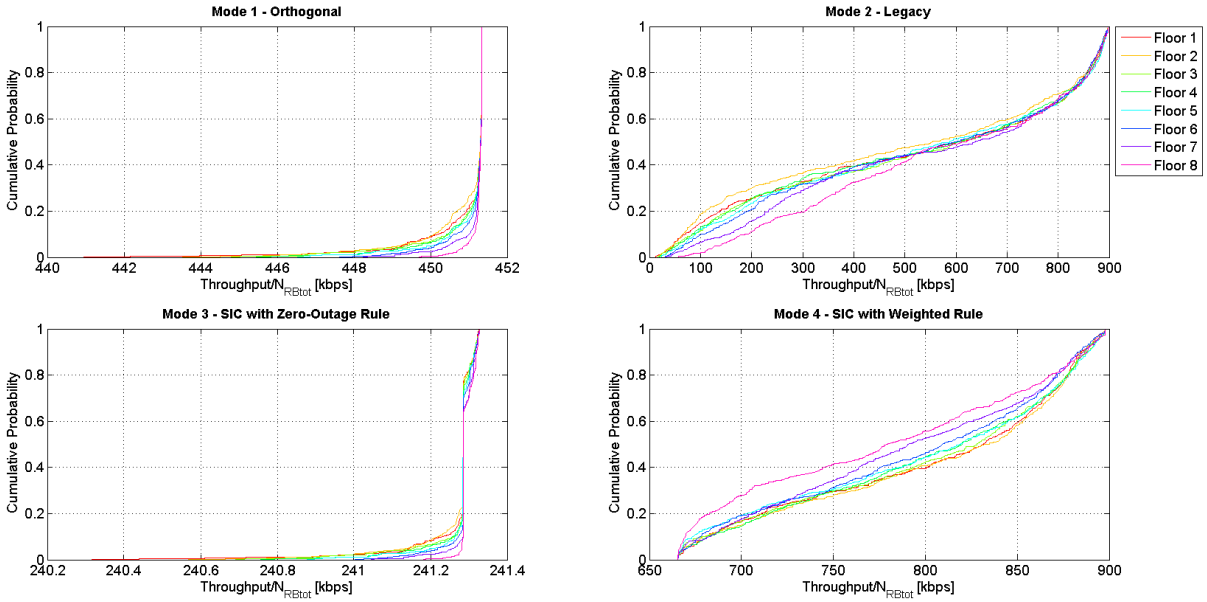

FIGURE 27. CDF OF I2D THROUGHPUT PER TOTAL RBS USED

Chapter 5. Conclusions and Future Work

5.1. Results Summary

Simulations carried in this work prove that the proposed rules meet the design criteria. Zero-outage rule focuses on combined link reliability by using robust MCSs. However, unlike the theoretical system where Gaussian codebooks are used [5], the fact that in LTE there is a discrete number of available MCSs, zero-outage is not achieved, but is significantly low. Indeed, on certain circumstances, this mode can even reach lower BLERs than that of orthogonal mode, despite in the former D2D and I2D links sharing the same resources. On the other hand, in zero-outage mode the efficiency is halved. However, the author cannot stress enough how important is, in the near future, sharing resources among several links due to the massive amount of active devices (M2M communications). So, in that sense, zero-outage rule is indeed a great tool to solve that incoming problem. Additionally, in such scenarios, estimating the CSI of D2D links in an accurate fashion might prove to be difficult and/or computationally intensive which further highlights the merit of this solution to the detriment of strategies such as weighted rule in which constantly knowing accurate estimates of D2D CSIs is of utmost importance.

Even though weighted rule tackles the LA problem in a heuristic fashion, hence being a suboptimal LA strategy, from all the evaluated methods, it is the mode that allows the highest combined throughput rates to be achieved so much so that it consistently exhibits double the performance than that of orthogonal mode. Despite not reaching BLERs as low as the zero-outage rule due to the usage of more efficient and less robust MCSs, its BLERs are not significantly higher. It should be stressed however that this strategy was evaluated under the assumption that there is perfect knowledge of CSIs. In real-life systems, this does not happen as not only the CSI estimation is prone to errors, the report of the CSI (via CQI in LTE) is also not instantaneous and occurs at periodic intervals. Moreover, noting that to compute the estimates, transmission is necessary to occur because it uses reference signals inserted in the resource grid, rules such as weighted rule suffer from some limitations. In fact, if D2D communications are to operate in an intermittent fashion, which in the context of M2M communications is likely to happen, allied to the presence of a fast fading channel, reported D2D CSI can be fairly outdated and thus highly inaccurate to the point of compromising the LA procedure if one is to use such information. Note that this does not mean that these type of rules are not applicable to real-life systems. In fact, the author believes that in sufficiently slow fading channels, weighted rule, despite being very simple to implement, might still yield a good performance.

5.2. Future Work

As previously stated, the LA strategies here devised can be applied to frequency selective channels with minor modifications, namely with the addition of a compression method (MIESM or EESM) to compute the effective SINR. Performance evaluation of the zero-outage rule and weighted rule under such channel conditions could then follow.

Alternatively, one could forego the assumption of an instantaneous CQI report and perfect channel estimation by applying a scheme that allows to model periodic CQI reports and channel estimation through the use of reference signals. The former would then imply the need for a new channel model in which correlation among channel coefficients exist. Slow and fast fading conditions, namely those standardized by 3GPP (EPA, EVA), could be evaluated. In the latter, it is the author's belief that zero-outage rule performance would not change significantly unlike weighted rule mode. In order to mitigate the problem of periodic CQI reports (periodic uplink frames), one could admit that instead of just sending one CQI report regarding the current CSI, the receiver would send several reports that span all the TTIs between upload frames. These CQIs would then be computed based on future CSI predictions by adding a filtering method, e.g. Kalman or particle filters. Similarly, the problem of intermittent D2D communications and the need to know the instantaneous D2D CSI could also be solved in a similar fashion. Evaluation of the performance and computational complexity would follow.

Other possibilities include the evaluation of these LA strategies for MIMO and/or the presence of multiple D2D links. In this case, reformulation of both strategies would be required. However, it is worth mentioning that for the particular case of multiple D2D links, a zero-outage rule that does not require D2D CSI knowledge cannot be devised because no positive downlink rate can ensure that the signal of the BS can be decoded [5].

References

[1] Cisco, "Cisco Visual Networking Index: Global Mobile Data Traffic Forecast Update, 2013–2018," 2014.

[2] S. Sesia, I. Toufik and M. Baker, LTE - The UMTS Long Term Evolution: From Theory to Practice, Wiley, 2011.

[3] F. Boccardi, R. W. Heath, A. Lozano, T. L. Marzetta and P. Popovski, "Five Disruptive Technology Directions for 5G," *IEEE Communications Magazine, Special Issue on "5G Wireless Communication Systems: Prospects and Challenges",* 2014.

[4] F. Gabor, S. Stefano and S. Shabnam, "Network Assisted Device-to-Device Communications: Use Cases, Design Approaches, and Performance," in *Smart Device to Smart Device Communication*, Springer, 2014.

[5] N. Pratas and P. Popovski, "Zero-Outage Cellular Downlink with Fixed-Rate D2D Underlay," 2014.

[6] 3GPP TS 23.401 v11.3.0, "General Packet Radio Service (GPRS) enhancements for Evolved Universal Terrestrial Radio Access Network (E-UTRAN) access," Release 11, 2012.

[7] 3GPP TS 36.300 v8.9.0, "LTE; Evolved Universal Terrestrial Radio Access (E-UTRA) and Evolved Universal Terrestrial Radio Access Network (E-UTRAN); Overall description," Release 8, 2009.

[8] H. Zarrinkoub, Understanding LTE with MATLAB: From Mathematical Modeling to Simulation and Prototyping, Wiley, 2014.

[9] 3GPP TS 36.212 v9.2.0 , "LTE; Evolved Universal Terrestrial Radio Access (E-UTRA); Multiplexing and Channel Coding," 2009.

[10] 3GPP TS 36.211 v11.1.0, "LTE; Evolved Universal Terrestrial Radio Access (E-UTRA); Physical channels and modulation," Release 11, 2013.

[11] Y. S. Cho, J. Kim, W. Y. Yang and C. G. Kang, MIMO-OFDM Wireless Communications with MATLAB, Wiley, 2010.

[12] 3GPP TS 36.213 v10.1.0, "LTE; Evolved Universal Terrestrial Radio Access (E-UTRA); Physical Layer Procedures," Release 10, 2011.

[13] S. Schwarz, C. Mehlfuhrer and M. Rupp, "Calculation of the Spatial Preprocessing and Link Adaptation Feedback for 3GPP UMTS/LTE," in *Wireless Advanced (WiAD), 2010 6th Conference on* , London, 2010.

[14] R. Irmer, H. Droste, P. Marsch, M. Grieger, G. Fettweis, S. Brueck, H. P. Mayer, L. Thiele and V. Jungnickel, "Coordinated multipoint: Concepts, performance, and field trial results," *IEEE Communications Magazine,* vol. 46, no. 2, pp. 102-111, 2011.

[15] D. Lee, H. Seo, B. Clerckx, E. Hardouin, D. Mazzarese, S. Nagata and K. Sayana, "Coordinated multipoint transmission and reception in LTE-Advanced: deployment scenarios and operational challenges," *IEEE Communications Magazine,* vol. 50, no. 2, pp. 148-155 , 2012.

[16] E. Hardouin, M. Hassan and A. Saadani, "Downlink interference cancellation in LTE: Potential and challenges," in *Wireless Communications and Networking Conference (WCNC)*, Shanghai, 2013.

[17] D. Tse and P. Viswanath, Fundamentals of Wireless Communication, Cambridge University Press, 2005.

[18] X. Zhang and M. Haenggi, "The Performance of Successive Interference Cancellation in Random Wireless Networks," 2014.

[19] J. Axnas, Y.-P. E. Wang, M. Kamuf and N. Andgart, "Successive Interference Cancellation Techniques for LTE downlink," in *Personal Indoor and Mobile Radio Communications (PIMRC), 2011 IEEE 22nd International Symposium on* , Toronto, 2011.

[20] METIS 2020 Project, 2014. [Online]. Available: https://www.metis2020.com.

[21] METIS, "Deliverable 6.1 - Simulation Guidelines," 2013.

[22] C. Mehlführer, M. Wrulich, J. C. Ikuno, D. Bosanska and M. Rupp, "Simulating the long term evolution physical layer," *Proc. of the 17th European Signal Processing Conference (EUSIPCO 2009), Glasgow, Scotland,* vol. 27, p. 124, 2009.

[23] S. Schwarz, M. Simko and J. C. Ikuno, "Vienna LTE Simulators Link Level Simulator Documentation, v1.7r1089".

[24] S. Schwarz, J. C. Ikuno and M. Simko, "Vienna LTE Simulators Link Level Simulator Documentation, v1.7r1089".

[25] Alcatel-Lucent, "DL E-UTRA performance checkpoint," 3GPP TSG-RAN1, Tech. Rep. R1-071967, 2007.

[26] S. M. Lopez, F. Diehm, R. Visoz and B. Ning, "Measurement and Prediction of Turbo-SIC Receiver Performance for LTE," in *Vehicular Technology Conference (VTC Fall), 2012 IEEE* , Quebec City, 2012.

[27] M. Mayer, M. Simko and M. Rupp, "Soft-output sphere decoding: Single tree search vs. improved k-best," in *Systems, Signals and Image Processing (IWSSIP), 2011 18th International Conference on* , Sarajevo, 2011.

[28] METIS, "Software implementation (Matlab) of PS3 and PS4," 2014. [Online]. Available: https://www.metis2020.com/wp-content/uploads/simulations/calclossPS3PS4.m.txt.

[29] 3GPP TR 36.931 v11.0.0, "LTE;Evolved Universal Terrestrial Radio Access (E-UTRA);Radio Frequency (RF) requirements for LTE Pico Node B," Release 11, 2012.

[30] K. Y. Yazdandoost and K. Sayrafian-Pour, "Channel Model for Body Area Network (BAN)," IEEE P802.15 Working Group for Wireless Personal Area Networks (WPANs), 2009.

Annex A

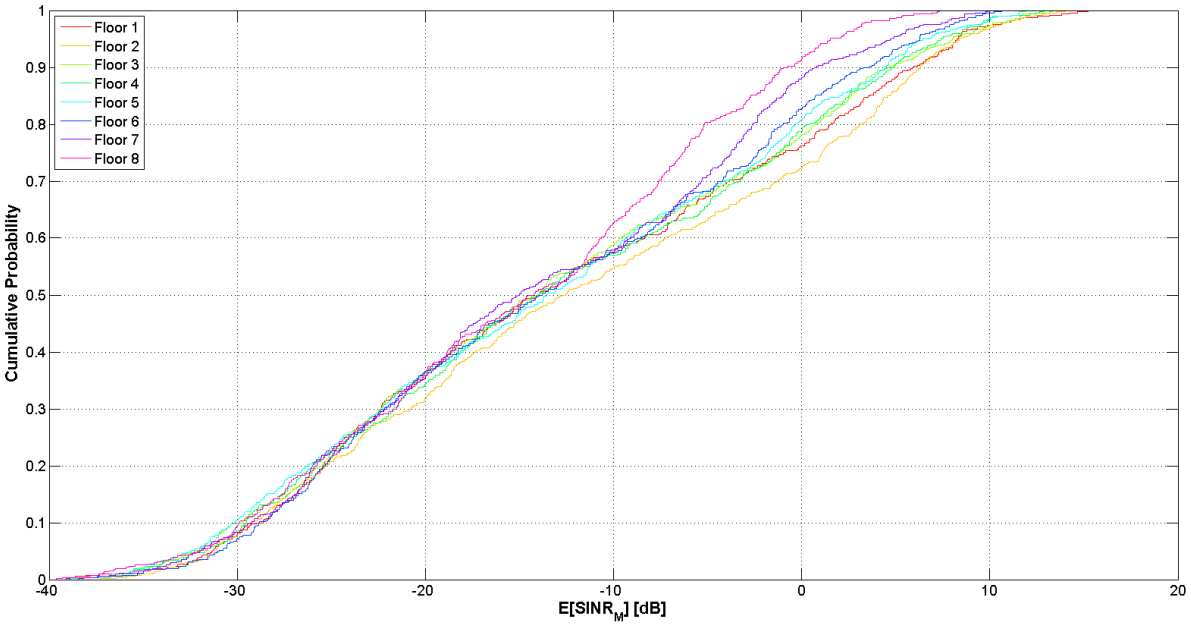

FIGURE 28. CDF OF D2D SINR

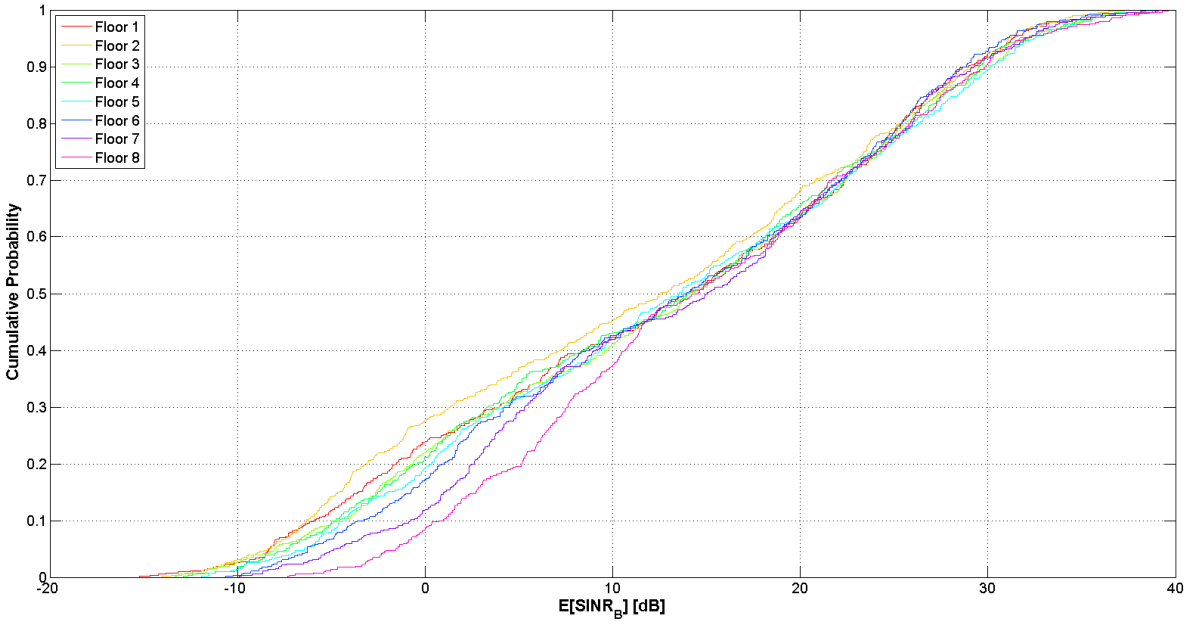

FIGURE 29. CDF OF I2D SINR

Annex B

Let $INR_i = \frac{SNR_i}{1+SNR_j}$, the author proves that $E[SINR_i] \geq \frac{E[SNR_i[k]]}{1+E[SNR_j[k]]}$.

First, note that $X \coloneqq SNR_i$ and $Y \coloneqq SNR_j$ are independent random variables that only take positive values. The expected value of $SINR_i$ can then be rewritten as:

$$E[SINR_i] = E\left[\frac{X}{1+Y}\right] = E[X]\ E\left[\frac{1}{1+Y}\right] \quad \textbf{(20)}$$

The second term inside the expectation operator is a convex function for the given domain (note that Y only takes positive values).

According to the Jensen's Inequality, if φ is a convex function and R a random variable then:

$$\varphi(E[R]) \leq E[\varphi(R)]. \quad \textbf{(21)}$$

Particularizing this inequality, one can write

$$\frac{1}{1+E[Y]} \leq E\left[\frac{1}{1+Y}\right], \quad \textbf{(22)}$$

and applying (22) to (20), one finally obtains

$$E[SINR_i] = E[X]\ E\left[\frac{1}{1+Y}\right] \geq \frac{E[X]}{1+E[Y]} = \frac{E\left[SNR_i[k]\right]}{1+E\left[SNR_j[k]\right]}. \blacksquare \quad \textbf{(23)}$$

Annex C

First, let the author determine the second order Taylor expansion of X/Y where X and Y denote positive-valued random variables (note that if Y had any nonzero probability of being 0 it would result in $E[X/Y]$ being undefined). Additionally, for ease of notation, let μ_K and σ_K^2 denote the expected value and variance of a generic random variable K. Next, applying the second order Taylor expansion around μ_X, μ_Y, one obtains:

$$\frac{X}{Y} \approx \frac{X}{Y}\Big|_{\mu_X,\mu_Y} + (X-\mu_X)\frac{\partial}{\partial X}\left(\frac{X}{Y}\right)\Big|_{\mu_X,\mu_Y} + (Y-\mu_Y)\frac{\partial}{\partial Y}\left(\frac{X}{Y}\right)\Big|_{\mu_X,\mu_Y} + \frac{1}{2}(X-\mu_X)^2\frac{\partial^2}{\partial X^2}\left(\frac{X}{Y}\right)\Big|_{\mu_X,\mu_Y} + \frac{1}{2}(Y-\mu_Y)^2\frac{\partial^2}{\partial Y^2}\left(\frac{X}{Y}\right)\Big|_{\mu_X,\mu_Y} + (X-\mu_X)(Y-\mu_Y)\frac{\partial^2}{\partial X \partial Y}\left(\frac{X}{Y}\right)\Big|_{\mu_X,\mu_Y} \quad \textbf{(24)}$$

After some algebraic manipulation and applying the expectation operator to the result:

$$E\left[\frac{X}{Y}\right] \approx \frac{\mu_x}{\mu_y} + \frac{\sigma_Y^2\mu_x}{\mu_y^3} - \frac{\sigma_{XY}}{\mu_y^2}, \quad \textbf{(25)}$$

where σ_{XY} denotes the covariance between X and Y.

Particularizing (25) to the case where $X = SNR_i$, $Y = 1 + SNR_j$ and SNR is defined as per (11) such that $h \sim \mathcal{CN}(0, 1)$, one obtains

$$E[SINR_i] = E\left[\frac{SNR_i}{1+SNR_j}\right] \approx \frac{E[SNR_i]}{1 + E\left[SNR_j\right]} + \frac{E\left[SNR_j\right]^2 E[SNR_i]}{\left(1+E\left[SNR_j\right]\right)^3}. \quad \textbf{(26)}$$

Equation (26) makes use of the fact that SNR_i and SNR_j are uncorrelated and that $|h|^2 \sim \mathrm{Exp}(1)$ which, in turn, means $\sigma^2_{|h|^2} = 1$, therefore:

$$\sigma^2_{1+SNR_j} = \sigma^2_{\left(\frac{|h_j|^2 P_j}{\sigma_w^2}\right)} = \sigma^2_{|h_j|^2}\left(\frac{P_j}{\sigma_w^2}\right)^2 = E\left[SNR_j\right]^2. \quad \textbf{(27)}$$